COMPARATIVE STUDY OF CO_2 CAPTURE USING ZEOLITE (ZSM-5) AND ACTIVATED CARBON FROM SUGARCANE BAGASSE

BY

ABUBAKAR, Onoruoiza Audu

MEng/SEET/2016/6145

DEPARTMENT OF CHEMICAL ENGINEERING

FEDERAL UNIVERSITY OF TECHNOLOGY
MINNA

NOVEMBER, 2019

ABSTRACT

The increasing energy demand can be meet globally with the use of non-renewable fossil fuels, however the use of these fossil fuels is associated with tremendous release of $CO_{2,}$ which largely contributed to greenhouse gases effect (GHG’s). Climate change or globally warning is one of the result of GHG’s effect, to prevent global warming or climate change, the excess amount of CO_2 in the atmosphere must be reduced to its bearable minimum, hence the need for carbon capture and storage techniques (CCS). CCS uses different solid adsorbents to remove excess CO_2 from the atmosphere which could be stored in aquifer or buried under the soil. In this work zeolite and activated carbon from sugarcane bagasse were used as an adsorbent for CO_2 adsorption from the atmosphere. The adsorption capacity of the adsorbents were determined and the result revealed that the amount of CO_2 adsorbed using activated carbon (65 mg/g) was higher than that of the zeolite (50 mg/g), however for both adsorbents, the adsorption capacity were higher than that of the commercial adsorbents when compared. The adsorption isotherm and kinetic models employed in this study revealed that the correlation coefficient, R^2 values of 0.9859 and 0.9691 respectively are close to unity, this closeness to unity indicates a favorable adsorption process. Increase in temperature from $25^{O}C$ to $100^{O}C$ was observed with a decrease in adsorption capacities of the adsorbents, whereas increasing the adsorbent dosage from 0.5g to 1.5g shows appreciable increase in the adsorption capacities of zeolite and activated carbon. The BET analysis on the adsorbents revealed the surface areas of $224.2m^2/g$ and $388.3m^2/g$ for activated carbon and zeolite respectively. The activation energy E_a of 15.3KJ/mol and 13.5KJ/mol for activated carbon and zeolite obeys physiosorption.

TABLE OF CONTENT

Content **Page**

CHAPTER ONE

CHAPTER TWO

CHAPTER THREE

CHAPTER FOUR

CHAPTER FIVE

REFERENCES

APPENDIX

LIST OF TABLES

Content **Page**

LIST OF FIGURES

CHAPTER ONE

1.0 INTRODUCTION

1.1 Background to the Study

The tremendous demand of energy in the world these days has caused the rising of greenhouse gases (GHG) emission, which is becoming the major concern by the public recently. Associated with that, carbon dioxide (CO_2) is labeled as the most important GHGs that contribute to the global warming through anthropogenic emission from power plant generation, transportation, and industrial sector (Rashidi *et al.,* 2014). Instead of adapting to the substantial effect of global warming, mitigation of the CO_2 emission is preferable. Therefore, immediate and continuous action should be taken to decrease the CO_2 concentration in the atmosphere. The CO_2 reduction can be done by some options such as an enhancement in combustion and energy efficiency, reduction in the use of fossil fuel, switch to non-carbon-emitting resources i.e. renewable energy, and to capture and sequester CO_2 (CCS) permanently. Amongst these options, CCS is considered as a useful technique, since it provides an ample time for the development of low-cost renewable energies and cleaner usage of fossil fuels resources during the transition period (Plaza *et al.*, 2007).

Among the possible technologies for CO_2 capture, solid adsorption is preferred due to low energy requirements, low capital and operating cost, together with limited secondary waste generation (Rashidi *et al.,* 2014). Activated carbon is one of the promising solid adsorbents that can be utilized to capture CO_2 due to its numerous benefits, such as inexpensive, easy for regeneration, insensitiveness towards the moisture, high CO_2 adsorption capacity at ambient condition, high specific surface area, adequate pore size distribution, high mechanical strength, as well as low energy requirement (Lua and Guo, 2001) .

In general, there are two main steps for the preparation of activated carbon (1) the carbonization of raw materials below 800 ^{o}C, in the absence of oxygen, and (2) the activation of carbonized product (char), either using physical or chemical activation methods (Sutrisno *et al.,* 2016).

Sugarcane bagasse (SCB) is suitable for preparing activated carbons due to their excellent natural structure and low ash content. SCB is a byproduct of sugarcane industries obtained after the extraction of juice for production of sugar. Conversion of sugarcane bagasse into activated carbons which can be used as adsorbents, ion exchange, carbon molecular sieve, catalyst would add value to these agricultural wastes help reduce the cost of waste disposal, and provide a potentially cheap alternative to existing commercial carbons. Studies on CO_2 adsorption using activated carbon from sugarcane bagasse have been reported in literature and hence the present study attempts to compare CO_2 capture using zeolite (ZSM-5) and activated carbon from sugarcane bagasse.

Several technologies to separate and capture the industrial emissions of CO_2 have been developed. Among them, certain technologies are based on the CO_2 adsorption/desorption by using natural, synthetic zeolites and activated carbon. The zeolites are a subclass of tectosilicates that possess a framework formed by a three dimensional assemblage of tetrahedra [SiO_4] and [(AlO_4)-] (Danielle *et al.,* 2008).

The CO_2 usually undergoes a physical adsorption (physisorption) at the surface of zeolites. The zeolites are recognized to be the potent CO_2 adsorbents that are able to adsorb and desorb CO_2. The adsorption capacity of zeolites depends on several factors including the size, polarizing power, distribution and the number of cations in their porous structure, Si/Al ratio, size, the form of their pores, the polarity and size of adsorbed molecules, the presence of water and other gas and presence of carbonates at their surface. Experimental conditions such as pressure and temperature are also among the factors influencing the adsorption capacity of zeolites. (Danielle *et al.*, 2008)

1.2 Aim of the Study

The research project is aimed at studying comparatively, CO_2 capture using zeolite (ZSM-5) purchased and activated Carbon produced from Sugarcane Bagasse.

1.3 Objectives of the Study

The aim will be achieved through the following objectives:

1. Production of activated carbon from sugarcane bagasse
2. Characterization of activated carbon and zeolite using SEM, FITR, BET and TGA.
3. Carrying out batch adsorption process to remove CO_2 using Zeolites and activated carbon from sugarcane bagasse.
4. Investigation on adsorption mechanisms, kinetics, and thermodynamic.
5. Comparison of the results from the two adsorbents

1.4 Statement of the Research Problem

Several authors have reported the use of activated carbon and zeolite as a good adsorbent for CO_2 capture, but the information about the comparison between activated carbon from sugarcane bagasse and zeolite (ZSM-5), to inform their choice in CO_2capture is limited, such information is what this research work seeks to address.

1.5 Scope of the Study

The scope of this work is limited to comparative study CO_2 capture using activated carbon and zeolites with varying adsorption variables such as initial concentration, contact time, temperature and adsorbent dosage at constant flowrate, as well as investigate the kinetics, isotherm and thermodynamic of the adsorption mechanism.

1.6 Justification of the Study

Comparison between activated carbon from sugarcane bagasse and zeolite in removing CO_2 will help to determine the best adsorbent suitable in removing excess CO_2 from the atmosphere.

CHAPTER TWO

2.0 LITERATURE REVIEW

2.1 Sugarcane

Sugarcane is a perennial grass that belongs to the poaceae family. The family consists of wheat, maize, rice, sorghum, etc. This family is very important owing to the fact that it serves as booster to so many economy around the world today. Sugarcane was labeled the largest crop in production in 2012 by the Food and Agriculture Organization, it states in her estimate that sugarcane is been cultivated on 26×10^6 hectares of land around the world in not less than ninety countries and in general (all around the world) harvest of $1.83\text{x}10^9$tons. (www.wikipedia.org/sugacanebagasse). The country with the largest production is Brazil, followed by other high level producers in decreasing order; India, China, Thailand, Pakistan and Mexico, respectively.

Table 2.1: Country and their production capacity of sugarcane

Country	Production capacity(thousand metric tons)
Brazil	739,267
India	341,200
China	125,536
Thailand	100,096
Pakistan	63,750
Mexico	61,182
Colombia	34,876

Indonesia	33,700
Philippines	31,874
United State	27,906
World	1,877,105

(Source: http://en.m.wikipedia.org/wiki/Sugarcane)

The title sugarcane holds as the largest produced crop is nothing compared to its recognized usage value, the sugarcane supply in the world is still less than its demand because of its so many uses. Sugarcane is used in the production of sugar, molasses, falernum, rum, cachaca, ethanol, spirit and bagasse. Larger percentage of the world sugarcane is used in sugar production.

2.1.1 Sugarcane bagasse

Sugarcane bagasse is a by-product gotten from sugarcane, as a result of the abundance nature of sugarcane; sugarcane bagasse is very well abundant and can be gotten in large quantity from the agro-related industries (especially the ones that use sugarcane as raw material). (Pereira *et al.*, 2011).

According to Suhardy and Nasery, (2005), 280kg of waste (sugarcane bagasse) is removed for 1 tons of sugarcane when sugar is extracted. Han *et al*., (1983) stated that more than 100 million tons of bagasse is produced all over the world and larger part of it are produced in the western hemisphere. Bagasse generally is regarded as the waste (fibrous in nature) that is generated after sugarcane is crushed, but the world we live in is one where some waste(or by-product) are almost useful in the same degree as the real product. Therefore bagasse is seen by some as the by-product or waste that causes environmental pollution (mostly in the underdeveloped or the third world countries). The same bagasse is seen by others as a resourceful material (countries with the appropriate technology to process it to useful commodity), (Pereira *et al.,* 2011).

Pereira *et al.,* (2011) and Concalves *et al., (*2005) carryout an analysis on "integrated process for conversion of sugarcane bagasse and straw" they concluded that "almost all products obtained from the petrochemical processes can be obtained from biomass through direct catalytic or aggressive conversion of cellulose, hemicellulose and lignin".

2.1.2 Composition of sugarcane bagasse

A lot of work (analysis) has been done on the subject, composition of bagasse. Sugarcane bagasse (mainly the ones from sugar production factories) has been confirmed to have good (high) level of moisture, around 40% - 50%, such high figure is not favorable in line with some of its uses, especially in the production of fuel. In the characterization of sugarcane bagasse, a work carried out by (Suhardy and Nasery, 2005). Sosa-Arnao *et al.,* (2004) stated that it is advantageous to dry sugarcane bagasse before use. Kim and Day (2011), did compositional analysis on Sugarcane bagasse and came out with a table shown below (values are average of six runs)

Table 2.2: Composition of sugarcane bagasse

Composition (dry bagasse)	Percentage (%)
Cellulose	41.6
Hemicellulose	25.1
Lignin	20.3
Ash	4.8

(Source: http://en.m.wikipedia.org/wiki/Sugarcane)

Pereira *et al.,* (2011) stated that cellulose and hemicellulose are hydrophobic. Sun *et al.,* (2004) stated that lignin and ash are hydrophobic. Han *et al.,* (1983) irradiated dry sugarcane bagasse and came up with a table of "Chemical composition of irradiated Sugarcane Bagasse (percent dry matter).

Table2.3: Chemical Composition of Irradiated sugarcane bagasse (percent dry matter).

Constituent	**Whole sugar bagasse**	**Fiber**	**Pith**	**NaOH extracted bagasse**	**H_2SO_4 extracted bagasse**
Cell-soluble matter	4.2	0.9	10.1	29.6	21.8
Hemicellulose	28.5	30.8	31.8	8.8	0
Cellulose	50.4	53.1	39.3	56.1	63.6
Lignin	14.9	13.3	15.3	4.9	22.5
Ash	2.0	1.8	3.2	0.4	0
Crude protein	1.59	1.31	1.85	0.23	1.01
Glucose yield by acid hydrolysis	4.4	4.4	5.0	6.0	4.0

Glucose yield by enzymatic hydrolysis	6.4	6.8	8.0	44.0	9.6

(Source: http://en.m.wikipedia.org/wiki/Sugarcane)

The components that make up bagasse are three in number, fiber, pith and rind, they are of different proportion. The shapes and sizes of these components are considerably different. The samples are approximated or modeled into our day to day shapes, pith as a spherical shape, fiber as a cylinder and rind rectangles.(Rudolph *et al.*, 1999).

2.1.3 Production, properties and storage

Sugarcane is a well cultivated plant around the world therefore bagasse follows inline, sugarcane harvesting and processing is mostly done around the last quarter of the year. Kim and Day (2011) stated (in her estimate) that the cost of harvesting and production of sugarcane in Louisiana is around $33 to $39 per ton. Sugarcane is most utilized in sugar production in USA, while in Brazil it is used in ethanol production, though they produce sugar as well.

Table 2.4: Typical features of sugarcane (Kim and Day, 2011)

Production Properties	**Sugarcane**
Crop cycle (months)	10-12
Number of crop cycle/years	1
Yield (t/ha/year)	70

Brix (%juice)	13-15
Fiber (%cane)	13.5
Fertilizer requirement (N:P:K)	2:1:1

(Kim and Day, 2011)

Table 2.4 talks about sugarcane production visibly but it also indirectly talks about bagasse production.

2.1.4 Uses of sugarcane bagasse

The world is gradually changing into one where there won't be any waste (if possible). Most technology been developed are directed towards waste utilization, even a lot of research are directed towards it. The growth in the industries (especially the agricultural industries) has led to the generation of quite a large number (millions of tons) of waste and by-products per annum (Chandel *et al.,* 2012). These waste or by-products have potentials to become materials for some other products, even though some are already in use, among those waste in use is the sugarcane bagasse. Sugarcane bagasse is used in the following areas: energy generation, production of biotechnology products, pulp and paper production, feed (human consumption) etc. sometimes these uses are classified in to Bio and Non-biotechnology applications.

2.1.4.1 Energy generation

In sugar mills (where sugarcane bagasse are mainly generated) sugarcane bagasse serve as an important fuel source, a large quantity of sugarcane bagasse is burned to produce enough energy (heat) needed and even more to sell for consumers. (Kim and Day, 2011) reported that steam and electricity are produce from burned bagasse. The worrisome aspect of this form of energy production is the emission of CO_2. CO_2 generated from bagasse burning process is well less when compared with amount absorbed by the plant (sugarcane) during its growth. Another aspect of energy generation (where bagasse is a raw material) is in the production of ethanol fuel. Ethanol production is from sugarcane and it is categorized under biotechnology application (Kim and Day, 2011).

2.1.4.2 Pulp and paper

The main raw material for the production of paper, board, tissue is wood, as the demand for these products increases and the need to retain trees in the forest arises researchers went to work and in the year 1937 a process for the production of paper from sugarcane bagasse was successfully developed, and in the year 2015, 90.000 metric tons of paper product was produced. (www.wikipedia.org/sugarcanebagasse).

2.1.4.3 Biotechnology application

Ethanol production falls under biotechnology application (Chandel *et al.*, 2012) reported that bagasse is a well-considered material in the biotechnology world, it is called “second generation ethanol”. Some other biotechnology applications of bagasse are as follows: production of xylitol, industrial enzyme, organic acids, antibihotics, single cell protein, bio-hydrogen, aroma, pigments. Before these products can be produced, bagasse passed through processes like, pretreatment, fermentation, enzymatic hydrolysis, and microbial fermentation.

2.1.4.4 Non biotechnology application

The activated carbon used in this work actually falls under this. A lot of products are gotten from bagasse through these processes: pyrolysis, chemical catalysis and chemical remediation, which are not biotech related. Some of this product are activated carbon, biochar coumaric acid, methyl cellulose, furfural and s-hydroxyl methyl furfural and pyrolysis and steam gasification (Chandel *et al.*, 2012).

2.1.4.5 Human consumption

Fibers gotten from bagasse are added to food for human consumption (www.nutrion411,com), it helps in intestinal regularity. "sugarcane bagasse is a unique source of organic fiber for use as a human dietary supplements" (Hsia, D.S, 2014) in his symposium "Backyard remedies". He also said that bagasse fibers help to prevent CV diseases, obesity, and diabetes (Type 2).

2.2 Activated carbons

Activated carbons are carbonaceous materials (Mendez *et al.*, 2006), It is predominantly an adsorbent with a large internal pore volume and surface area (Bansode *et al.,* 2003), it is a unique and versatile adsorbent because of its microporous structure (Nakagawa *et al.*, 2003), Its pore volume typically ranges from 0.20 to 0.60 cm^3/g, and has been found to be as large as 1 cm^3/g. Its surface area ranges typically from 800 to 1500 m^2/g (Bansal and Goya, 2005), but has been found to be in excess of 3,000 $m^2/$ g. The surface area contains mostly micropores with pore diameters smaller than 2 nm (Beguin and Frackowiak, 2010), it has high adsorption capacity, and high degree of surface reactivity (Williams and Reed, 2006). These favorable properties make activated carbon a popular adsorbent for many applications.

(Leimkueler *et al.,* 2010). Activated carbons can be produced from a number of precursor materials including wood, agricultural wastes, coal and synthetic resins (Sivakumar *et al.,* 2012). It is most commonly derived from charcoal (Michael *et al.,* 2004). Some of the agricultural waste according to researchers that AC can be gotten from are palm-tree cobs (Daud *et al.,* 2000), cassava peel (Rajeshwarisivaraj *et al.,* 2001), bagasse (Tsai *et al.,* 2001), jute fibre (Senthilkumar *et al.,* 2005), coconut husk (Tan *et al.,* 2008), seed shells (Thinakaran *et al.,* 2008), cocoa shell (Theivarasu *et al.,* 2011) and Eucalyptus globules Bark (Kannan *et al.,* 2012). Numerous low cost alternatives have been proposed as good materials to get activated carbon, they include sago waste (Kadirvelu *et al.,* 2005), waste coir pith (Namasivayam *et al.,* 2001), pine sawdust (Ozacar and Sengil, 2005), rubber wood sawdust 6 (Vasanth and Sivanesan, 2007), bottom ash and de-oiled soya (Gupta *et al.,* 2006). In recent years, a number of adsorptive material, tea factory waste and sheep manure waste are also seen as good precursors. AC can be produced by any one of the following processes described below:

a. Physical activation:

   By this process of physical activation, precursor is developed into activated carbons using gases. This is generally done by using one or a combination of the following processes: Carbonization or Activation (oxidation). In Carbonization, Material having appreciable carbon content is pyrolyzed at temperature ranging between 600–900°C, in the absence of oxygen (usually in inert atmosphere with gases like argon or nitrogen). In Oxidation, raw material or carbonized material is exposed to oxidizing atmospheres (carbon monoxide, oxygen, or steam) at temperatures above 250°C, usually in the temperature range of 600 to 1200°C.

b. Chemical activation:

Before carbonization, the raw material can be impregnated with certain chemicals (Srinvaskannan and Mohammed, 2004). The chemical needs to be typically an acid, strong base, or a salt (phosphoric acid, potassium hydroxide, sodium hydroxide, zinc chloride, respectively). After impregnation, the raw material needs to be carbonized at lower temperatures (450–900 °C). It is believed that the carbonization / activation step proceeds simultaneously with the chemical activation. Chemical activation is preferred over physical activation owing to the lower temperatures and shorter time needed for activating material (Sua“rez-Garcci“a *et al.*, 2002). The surface oxygen functional groups can be easily introduced to the carbon by different activation methods including dry and wet oxidizing agents.

Dry oxidation methods involve the reaction with hot oxidizing gas such as steam and CO_2 at temperatures above 700 0C (Smisek and Cerney, 1970) Wet oxidation methods involve the reaction between the carbon surface and solutions of oxidizing agents such as phosphoric acid H_3PO4, nitric acid HNO_3, hydrogen peroxide H_2O_2, zinc chloride $ZnCl_2$, potassium permanganate $KMnO_4$, ammonium persulphate $(NH_4)_2SO_8$, potassium hydroxide KOH, etc. From the above oxidizing agents, phosphoric acid and zinc chloride are usually used for the activation of lignocellulosic materials, which have not been carbonized before (Puziy *et al.*, 2006). On the other hand, potassium hydroxide is usually used to activate coal or chars precursors. It has been reported that zinc chloride produces activated carbon with higher specific area than that produced by using phosphoric acid (Thomas *et al.*, 1997).

However, phosphoric acid activation is widely preferred over zinc chloride because $ZnCl_2$ has bad environmental impact and the activated carbon produced when using it cannot be used in the food and pharmaceutical industries (Srinivasakannan and Abu, 2006). Activated carbon usually increases the cost of the treatment process. Its economical drawback has stimulated the interest to utilize cheaper raw materials for the production of activated carbon (Rengarag *et al.*, 2002).

Adsorption of activated carbon is governed by the chemical nature of the aqueous phase, the solid phase, and the chemical nature of the adsorbing organic (Bilal *et al.,* 1996). According to Torregrosa-Macia *et al.* (1997), for a given industrial application, a solid adsorbent with a relatively wide pore size distribution can be obtained solely through a chemical activation process.

Physical activation can further enhance the adsorbent‟s pore structure due to a partial oxidation of the carbonized material by gases such as CO, CO_2 or steam (Molina-Sabio *et al.,* 1996). Analysis of the surface physical properties of the carbon includes determination of the total surface area, extent of microporosity, and characterization of the pore size distribution (Rodriguez-Reinoso *et al.,* 1995). Nitrogen adsorption isotherms are commonly used for these types of surface analyses. The measured relative pressure and adsorbed volume of nitrogen gas are commonly used in various mathematical models that is Brunaer Emmett Teller (BET) model to calculate the monolayer coverage of nitrogen adsorbed on the adsorbent surface, while the characteristics of the pore structure and pore distribution can be identified from comparative plots such as ‗t„ and ‗αs„-plots (Aranovich and Donohue, 1998).

The extent of the microporosity is commonly evaluated by applying low-pressure isotherm data to the Dubinin– Radushkevich (DR) equation. The pore size distribution and the corresponding surface areas of the mesoporous adsorbents are traditionally calculated from the hysteresis loop according to the BJH theory, which is based on the Kelvin equation. The useful properties of activated carbon have been known since ancient times. This traces back to 1500 BC when Egyptians used charcoal as an adsorbent for medicinal purposes and a purifying agent. Around 420 BC it was observed that Hippocrates dusted wounds with powdered charcoal to remove their odor. Ancient Hindu societies purified their water by filtration through charcoal (Bansal *et al.,* 2005). In 1773, the Swedish chemist Karl Wilhelm Scheele was the first to observe adsorption of gases on charcoal. A few years later activated carbons began being used in the sugar industry as a decolorizing agent for syrup. In the early 20th century the first plant to produce activated carbon industrially was built for use in sugar refining industry in Germany.

Many other plants emerged in the early 1900"s to make activated carbons primarily for decolourization. During World War I activated carbon was used in gas masks for protection against hazardous gases and vapors. Today, activated carbons are used to remove color from pharmaceutical and food products, as air pollution control devices for industrial and automobile exhaust, for chemical purification, and as electrodes in batteries. 500,000 tons per year of activated carbon are produced globally. (Jankowska *et al.,* 1991) 80 % of this is used for liquid phase applications, and 20 % is used for solid phase applications. Over the years, many works have been carried out on the production of Activated Carbon. Alaya *et al.,* (2000) carried out an investigation on the Adsorption Properties of Activated Carbons Prepared from Olive Stones by Chemical activation using zinc chloride (25– 50 wt %) or by gasification with steam to burn-offs between 25 and 49 %. They discovered that Chemical activation produces physical and chemical changes which lead to modification of the process of thermal degradation.

Steam activation to low burn-offs created new micropores, while such activation to high burn-offs led to widening of the existing pores. Cuhadaroglu and Uygun, (2008) carried out a research on the production and characterization of activated carbon. In their study, the use of bituminous coal as a precursor for the preparation of activated carbons using KOH, NaOH and other chemical reagents was analyzed in detail. The influence of several variables such as impregnation ratio and carbonization temperature was studied. In the first group of experiments, in which the impregnation ratio between the chemical reagent and the precursor were 4/4, 2/1, 1/1, they found out that BET surface areas change between 1295 and 785 m^2/g for KOH activated carbons and 1566 and 657 m^2/g for NaOH activated ones. BET surface areas and total pore volumes of KOH activated active carbons are higher than that of NaOH activated ones.

They also discovered that increasing the amount of activating reagent (increasing impregnation ratio) has another effect; the activation level is also increased, but the resultant pore texture is different. According to the results of the second group of experiments, in which the impregnation ratio is fixed to 1/1 to determine the effects of carbonization temperature, activation level increases with increasing temperature up to 900 ºC but it decreases over 900 ºC for active carbons obtained by KOH. For active carbons obtained by NaOH, increasing the carbonization temperature raises the activation level. Activated carbon with a BET surface area from 1596 - 1015 m^2/g were obtained by activation with KOH, 1461 to 945 m^2/g were obtained by activation with at NaOH at an impregnation ratio between chemical reagent and precursor: 1/1. When FTIR spectrum at 1000 ºC is compared, it shows that the degree of carbonization is higher for the sample activated by NaOH as it can be appreciated by the lower intensity of the O-H band at 3422 cm-1. Ruiz *et al.,* also, did an investigation in 2014 on the production and characterization of activated carbon from oil-palm shell for carboxylic acid adsorption. In their study, the recovery of shortchain carboxylic acids was explored by adsorption onto activated carbon from palm-oil kernel shell using H_3PO_4 and KOH as activating agents.

The surface of activated carbons was characterized physically and chemically. An adsorption-desorption study was performed finding that carbon CA60B exhibits greater adsorption capacity (1300 mg of adsorbed acids/g carbon or 33.3 % of acids present in the solution), CA10A and CA60A present an acidic surface with pore diameter between 1-4 nm. CA10B y CA60B present a basic surface with pore diameter between 0.96-5 nm. Five adsorption isotherms models were fitted to experimental data where the Langmuir-Freundlich model described best the adsorption phenomena. The adsorbent CA60B presented a higher amount of acid desorbed by temperature change (44.1mg of carbon desorbed for initially containing 276mg of acid). Hariprasad *et al.* (2016) carried out an experiment on the preparation and characterization of activated carbon from rice husk. In their experiment, activated carbon was prepared from rice husk and its characteristics were investigated.

The materials selected were initially physically activated at temperature ranging from 300 to 700^{O}C in muffle furnace with a holding time of 1hr and the carbonized material thus obtained was soaked in 1N KOH, in 1:1 ratio for overnight and was followed by physical activation at 300^{O}C for 2hrs in muffle furnace. The activated carbon they obtained was found to be ranging from 11.9985 to 279.7752 m^2/g and the pore sizes were found to be 13.3909 to 15.4260 Å. They also found out that the pore diameters of rice husk activated carbon were increasing (13.3909 to 15.4260 Å) when the activation temperature was increased. Surface analysis of activated carbon was done by scanning electron microscopy (SEM), FTIR analyses in order to identify the appearance and disappearance of functional groups during different activation temperatures. From the data they obtained, rice husk activated carbon obtained at 600 ^{0}C could be used as a low-cost adsorbent with favorable surface properties. The usefulness of carbon or carbon related materials cannot be over emphasized; its abundance (by mass) is ranked as the fourth in the universe.

Activated carbon is a processed carbon, a carbonaceous substance that has very different structure when compared to its primary raw material (complex structure); it has interconnected pores within its layers which are established by the activation process, the pores are connected by chemical bonds. These pores leads to its high porosity level (www.haycard.com/activated-carbon). The main two processes involved in the production activated carbon are pyrolysis and activation. When activated carbon is produced on a large scale using high-cost raw material like wood, petroleum and coal, it leads to an unjustified ending in pollution control. Nowadays as a result of the fruitful effort of researchers all around the world, activated carbon has become one of the materials with least expensive raw material (mostly agricultural waste). Some of the materials used in producing activated carbon are bagasse, coconut shell, sawdust, rice straw, jatropha seed, oil palm fiber, etc. (AlOthman *et al.*, 2011).

The need for very less expensive raw material for activated carbon arises from the fact that pyrolysis and activation process will always have a very low yield (Shah, 2007). He also recorded that the kind and level of processes used in pyrolysis and activation and the cost of raw material are the determinant of the final sales price of the product.

Table 2.5, contains the list of the raw materials used in the production of activated carbon and percentage usage (in commercial production).

Table 2.5 : List of raw materials used in activated carbon production

Precursor	Use %
Wood	35
Coal	28
Lignite	14
Coconut shell	10
Peat	10
Others	3

(Shah, 2007)

Activated carbon has a lot of attractive properties, the main determinant of these properties are the technology used in the production and the nature of the raw material (Shah, 2007).

2.3 History of activated carbon

Activated carbon has a very long history, Cameron-carbon Incoporated, (2006) stated that the ancient Egyptians uses activated carbon in the purification of oil and in medicine. Kirk-Othmer and Encyclopedia (2014) recorded that activated carbon (in the form of charcoal) can be traced back to the prehistoric age and it states a number of ways in which it has been utilized from around 8000 BC to the 18th century and also its uses nowadays. Leimkuehler (2010), could trace it back to 1500 BC in the old Egypt and he talked about its uses down the line. Activated carbon is a product that a very deep and rich history, however (Silvestre-Albero *et al.,* 2016) recorded that large scale production of activated carbon commenced in the 20th century and the rise of the world war 1 also gave rise to better production. i.e development in its technology. After this activated carbon begins to find its foot and it became very popular in taking care of pollution. Recently activated carbon establishes itself (through researches) as a good impurity remover.

2.3.1 Production of activated carbon

As earlier said a lot of materials can be used in activated carbon production (carbonaceous materials though). According to Cameroncarbon Incoporated, (2006) , 300,000 tons of activated carbon are produced manually.

2.3.1.1 Factors affecting production

The following represent the factors upon which production of activate carbon rest on:

Raw material

A lot of precursors could be used in activated carbon production, in order to select the best raw material for an activated carbon production (e.g. adsorption capacity, adsorption mechanism etc.) a number of factor must be considered, these are:

- The carbon content
- The stability of supply
- The extent of activation
- The cost
- The density and sufficiency of the volatile content
- The ash content

Temperature

The properties or characteristics of the final product (activated carbon) are affected by the final activation temperature, for some commercial production, they are activated at 800^{o}C. The yield and surface area is well affected by the activation temperature. The optimum temperature has been found to be in the range of 400^{o}C – 500^{o}C (Jabit, 2007). Lua and Guo, (2001) reported that the yield reduces when activation temperature is increased because more volatile substances are expelled. Jabit, (2007), in his work recorded that increasing the carbonization temperature reduces the volatile matter present. The activation temperature and carbonization temperature are strong factors to be considered in the production of activated carbon.

Activation time

The properties and characteristics of activated carbon, even the carbonization process is affected by the activation time. The time is inversely proportional to the yield percentage but directly proportional to the BET surface. Kim *et al.,* (2011), recorded that the gravity of the reduction in product yield is noticed when there is excessive activation as stated by (Jabit, 2007).

2.3.2 Structure

Activated carbon has a porous structure, its structure has its origin from a very faulty form of graphite lattice, which is similar or equivalent to a carbon that is non-graphatizable. The structure of the polymer that make up the raw material does not change when been treated with heat, it only lost some molecules through degradation. When crosslink happens it prevent fusion and causes a rigid structure product that is almost immobile which dis allow the proper arrangement when graphitization is taking place, this leads to the porous structure. Pyrolysis leads to the carbon atoms in the precursors being arranged to form a shape of aromatic sheets linked (cross) together. The char formed is not in a regular manner which leaves some pours between them. The irregularity of these carbon present in the char goes into reaction with gases when activation is being carried out which leads to the porosity of activated carbon.

Figure 2.3 : microstructure of activated carbon, (Silvestre-Albero, 2016)

As stated by IUPAC, three kinds of pores are present in an activated carbon, the micropore, mesopores and the nanopores. Though the micropores are the most important (adsorption mostly take place there). The mesopore and micropore is a road that leads to the micropores. The porosity of any activated carbon depends on the raw material, how its been prepared, how its been activated and how long it was activated. Therefore the pore volume and surface area of finished activated carbon differs (Silvestre-Albero, 2016).

2.3.3 Manufacture

Activated carbon mainly comes (manufactured) in two physical forms which are powdered and granular. According to Silvestre-Albero (2016) the production capacity of activated carbon in the year 2014 was estimated to be more than 1.5 x 10^6 tons per annum, which is expected to increase (more than 10% per annum) with time. Activated carbon can be produced through two processes: chemical and physical activation.

2.3.4 Test for activated carbon

After the production of activated carbon the characteristics of the product must be determined, the properties of the product are necessary for both the user and the producer. The adsorptive properties, chemical properties, physical properties, and mechanical properties, are tested when characterization is done on the activated carbon. A lot of test methods for the characterization of products are available in the literature e.g. iodine adsorption test, methylene blue adsorption test, butane adsorption test, dynamic test, molasses decolonization test etc.(Silvestre-Albero, 2016).

CHAPTER THREE

3.0 MATERIALS AND METHODOLOGY

3.1 Materials

Activated carbon produced from sugarcane bagasse was used in this work. Gaseous CO_2 was purchased from gas deport in Minna Niger state. The adsorption column used was gotten from chemical engineering laboratory and the zeolite used was also gotten from the department.

3.2 Synthesis of activated carbon from sugarcane bagasse

The activated carbon used in this work was prepared and made available.

The schematic diagram in figure 3.1 shows the step in production of activated carbon used in the present work.

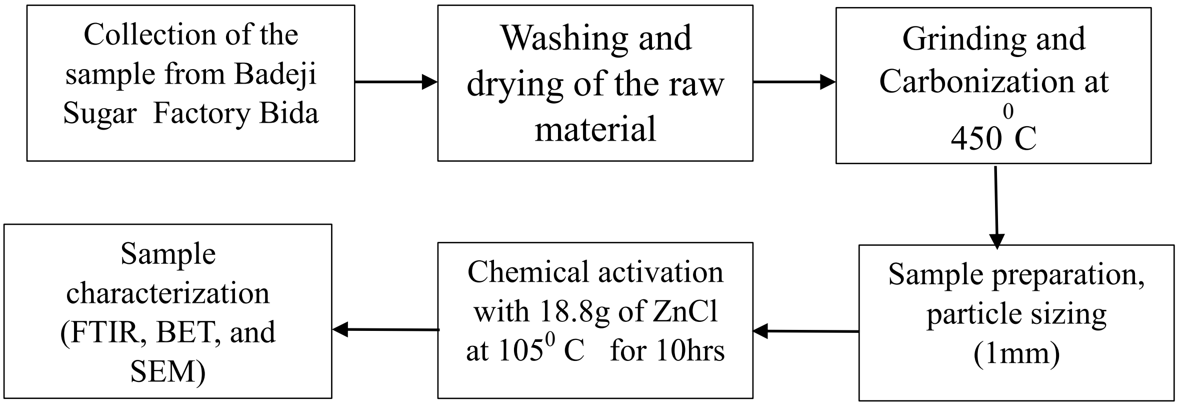

Figure 3.1: Schematic representation of the preparation of activated carbon from sugarcane bagasse

The Sugarcane bagasse used was collected from Badeji sugar factory, Bida. The bagasse was thoroughly washed to remove any debris present, and then it was sundried for about five days. The bagasse was grinded using a ball grinder, and oven dried at a temperature of 150^oC. The powdered bagasse was sieved to give an under-size of 1mm which was used. The sample was washed with distilled water to remove unwanted materials which was separated as filtrate. The washed bagasse was impregnated with 18.8 g of ZnCl for 10hours, after which it was washed with distilled water and dried to remove moisture. The dried weight before carbonization is 1,582.07 g, the weight after carbonization is 579 g and the weight after activation is 417 g. The bagasse was carbonized at a temperature of 450^oC and the activation was carried out at 105^oC. The surface area of the final Activated carbon is 224.2 m^2/g and the pore volume is 0.1363 cc/g.

3.3 Zeolite

The zeolite used in this work is Zeolite Ammonium ZSM-5 (Zeolite Socony Mobile-5) powder which was purchased, were produced by Zeolyst International. It is a white odorless powder, with surface area is 388.3 m^2/g and an estimated pore volume of 0.1363 cc/g.

3.4 Preparation of equipments

The adsorption column, the beaker, the spatula, the cork and the two delivery hose were washed with detergents, at the completion of the washing they were properly rinsed and placed in warm water. This was done because some of the apparatus has been left in the open for a while (especially the adsorption column) and also to avoid any form of impurity whatsoever.

Table 3.1 List of materials and equipment

Equipment	Manufacturer	Source
Digital weighing balance	Ohaus cooperation	Chemical Engineering Department, FUT Minna
Beakers	Pyrex (England)	Chemical Engineering Department, FUT Minna
Cylindrical adsorption	Pyrex (England)	Chemical Engineering Department, FUT Minna
Column	Pyrex (England)	Chemical Engineering Department, FUT Minna

3.5 Experimental variables

In order to analyze the effectiveness of a particular substance or material (e.g. activated carbon), the totality of the factors responsible for its workability must be tested. This analysis helps to determine and establish the optimum time, temperature and adsorbent dosage where the effectiveness of the activated carbon achieves the highest efficiency. Therefore in this work the CO_2 adsorption experiment was carried out by maintaining the flow rate of CO_2 into the adsorption column at 1 m/min, and varying the bed height 2.7, 5.4, and 8.1 cm which represents 0.5, 1 and 1.5 grams of the activated carbon in the adsorption column and the time taken for the adsorption process to be carried out.

After a successful experiment has been carried out, how sure is the analyst that the results of the experiment are actually correct? Through comparison with the literature, control experiment and the results of other people who has carried out same experiment or a very close experiment and which has been certified correct. This same experiment will be carried out using zeolite (with other variables, experimental conditions and procedure the same as that of sugarcane bagasse activated carbon).

3.6 CO_2 Adsorption experiment (activated carbon)

The gas adsorption column used in this experiment is cylindrical in nature, the adsorption column was held by a standing wooden support, the hose delivering CO_2 (from the gas cylinder) is connected to the base end of the column, the other end of the column i.e. the upper part has an open end where an exit hose can be fitted, the open end was well corked and an exit hose was connected through the opening at center of the hose. (Alhassan *et al.,* 2017).

With the aid of an analytical weighing balance 0.5g (2.7 cm bed height) of activated carbon were measured and placed in the column (with a foam support) and the gas cylinder's tap was opened at 1L/min and the time of adsorption was varied from 10 to 60 mins till equilibrium is achieved. This operation was carried out at atmospheric pressure and room temperature 25^{o}C. The same operation was repeated for 1g and 1.5g (5.4 and 8.1 cm bed heights) of activated carbon. The weight of the activated carbon samples were measured at the end or every run (i.e. 10 min) to ascertain the difference in weight of the activated carbon (sample) in other to determine the amount of CO_2 that has been adsorbed and to determine how long it will take the activated carbon to reach its maximum capacity.

Figure 3.3: Experimental setup for CO_2 Adsorption

3.7 CO_2 Adsorption experiment (Zeolite)

The experiment was like a repetition of the one carried out using the sugarcane bagasse activated carbon. All the procedure was followed to the tiniest detail, only that there was a change in the adsorbent used i.e. zeolite was used this time.

Amount of CO_2 adsorbed = $\frac{\mathrm{Mt(mg)–Mo(mg)}}{Mo(g)}$ 3.1

Where:

M_o = initial mass before adsorption

M_t = final mass after adsorption

3.8 Adsorption Isotherm

This is a way to represent the variations (isothermal) found in adsorption experiment i.e. the variation in the quantity of adsorbate taken up by an adsorbent at constant temperature and at the equilibrium pressure of the adsorbed gas. Several isotherm models are used for predicting the adsorption equilibrium distribution, the Langmuir, Freundlich and Temkin isotherm models were used in this analysis, to model the experimental data recorded.

Langmuir:

$$\frac{p}{q_e} = \frac{1}{q_m} + \frac{1}{k_{1\,q_m t}} \qquad 3.2$$

Where: q_e is the amount adsorb at time t

T is the Adsorption Time (min)

K_1 is the Langmuir Rate Constant

P is Atmospheric Pressure

Plot $\frac{1}{q_e}$ Vs $\frac{1}{t}$

Slope = $\frac{1}{k_{1\,q_m}}$

Intercept = $\frac{1}{q_m}$

Freundlich:

$$\log(\mathcal{X}/m) = \log k_f + \frac{1}{n}\log t \qquad 3.3$$

Where $\mathcal{X}/m = G_t$

Plot log $(\mathcal{X}/m)$ Vs log t

Where: q_e = amount adsorbed at time t

T = adsorption time

K_f = freundlich rate constant

Slope = $\frac{1}{n}$

Intercept = log k_f

Temkin Isotherm:

Q_e = In K_1 + B In t_e 3.4

Where: B is Slope from the Plot

K_1 Temkin Rate Constant

T_e is Adsorption Time

Q_e is Amount Adsorbed of Time t.

Plot q_e Vs In t_e

Slope = B

Intercept = B In k_1.

These constant values depend on the type and nature of adsorbate, adsorbent and temperature. A plot of p/(x/m) against p and log x/m against log p were plotted and the intercept and slope is obtained which are in turn used to determine the constants.

3.9 Adsorption Kinetics

A lot of kinetic models exist which can be used in the modeling of gas adsorption (using activated carbon), some of which are Lagergren's pseudo-first order, Lagergren's pseudo-second order, Elovich, intra-particle diffusion, BVM etc. Abia and Asuquo,(2005) recorded that some factors (in independent processes) could control adsorption kinetics such as diffusion (bulk, film and intra-particle), chemical reaction, temperature etc. as stated in (Ifechukwu G. *et al.*, 2016). The kinetic and equilibrium data generated in this work is fitted using the Lagergren's pseudo-first order, the Lagergren's pseudo-second order models and the intra-particle diffusion (Alhassan *et al.*, 2017). Regression coefficient (R^2) value is a good accuracy test tool which helps in testing the conformity of the experimental result in this work (Adilla *et al.*, 2013)

Table 3.2: The Lagergren kinetic equations

Kinetic equation	**linear form**	**Plot made**
Pseudo-first order	$\log(q_e - q_t) = \ln q_e - k_1 t$	$\log(q_e - q_t) \text{vs.} Time$
Pseudo-second order	$\frac{t}{q_t} = \frac{1}{(k_2^2 q_e^2} + \frac{t}{q_e}$	t/q_t vs. Time
Intra-particle diffusion	$q_t = kt^{\frac{1}{2}} + C$	q_t vs time$^{\frac{1}{2}}$

(Singh and Kumar, 2015)

Where:

$\mathrm{q_e}$ in mg/g represent the quantity of CO_2 adsorbed at equilibrium $\mathrm{and}\,\mathrm{q_t}$ represent the quantity of CO_2 adsorbed at time t, C is the thickness of boundary layer, k_1 in (min^{-1}) and k_2 in (g/mgmin) represent the pseudo-first order and pseudo-second order rate constants, k in (mg/gmin$^{1/2}$) represent the diffusion rate. The plot of $\log(\mathrm{q_e} - \mathrm{q_t})\mathrm{vs.\,Time}$ gives $k_{1,}$ that of $\mathrm{t/q_t\,vs.\,Time}$ gives $k_{2,}$ while that of qt vs. time$^{1/2}$ gives k. slopes and intercepts of all the plots were evaluated.

CHAPTER FOUR

4.0 RESULTS AND DISCUSSION

4.1 Characterization of Adsorbents

Characterization of the activated carbon and zeolite were examine using TGA, FTIR, SEM and BET.

4.1.1 Thermo-gravimetric analysis (TGA)

Figure 4.1a and 4.1b shows the thermo- gravimetric analysis for activated carbon and zeolite respectively. These adsorbents were measured continuously while heating. There was a steady decomposition (loss of mass) of adsorbent from 50 to 200^{O}C and a rapid loss of mass between the temperature of 220 to 300^{O}C for activated carbon and 300 to350^{O}C for zeolite.

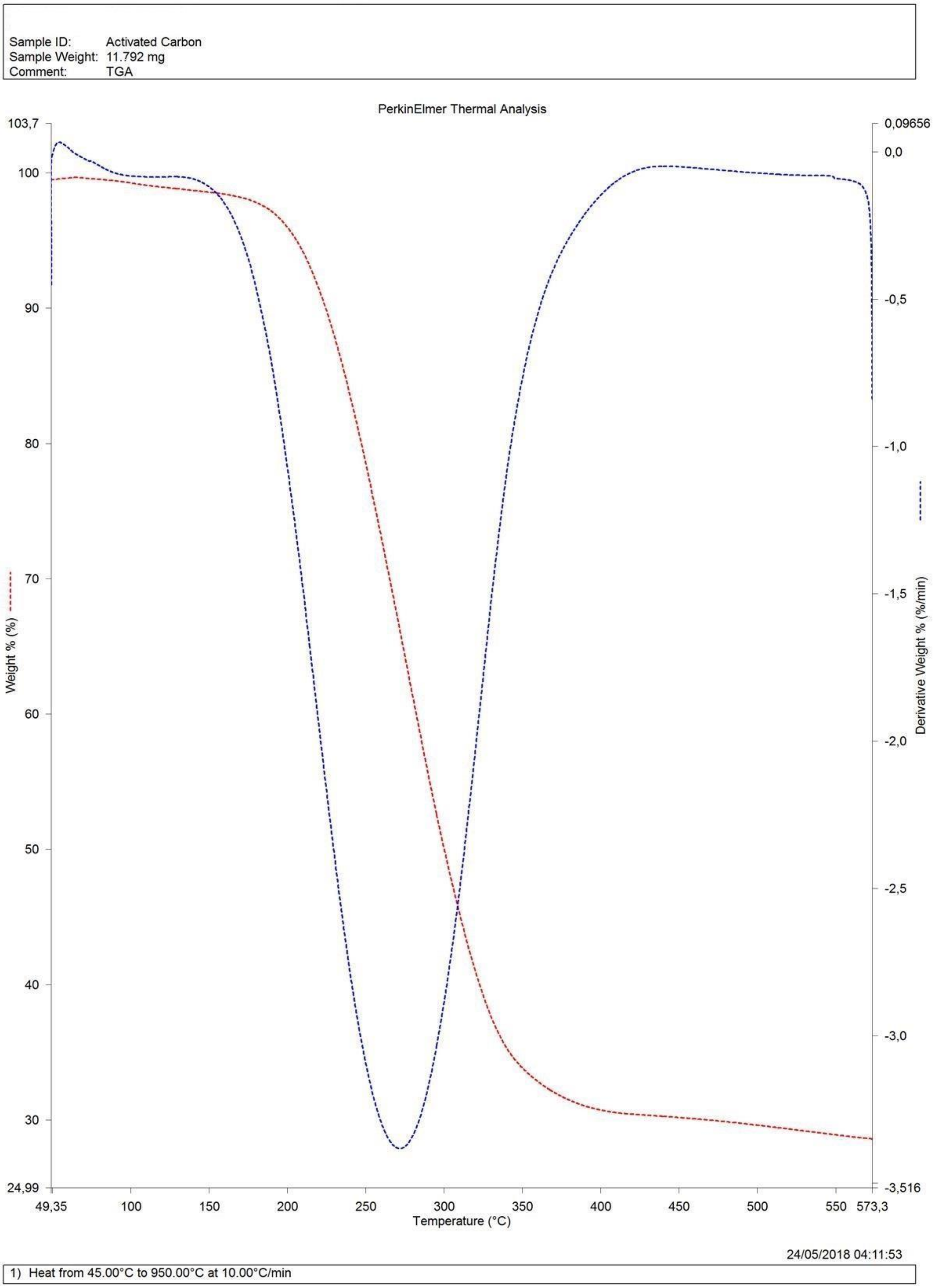

Sample ID: Activated Carbon
Sample Weight: 11.792 mg
Comment: TGA

1) Heat from 45.00°C to 950.00°C at 10.00°C/min

Figure 4.1a: TGA/DTA before adsorption (Activated carbon)

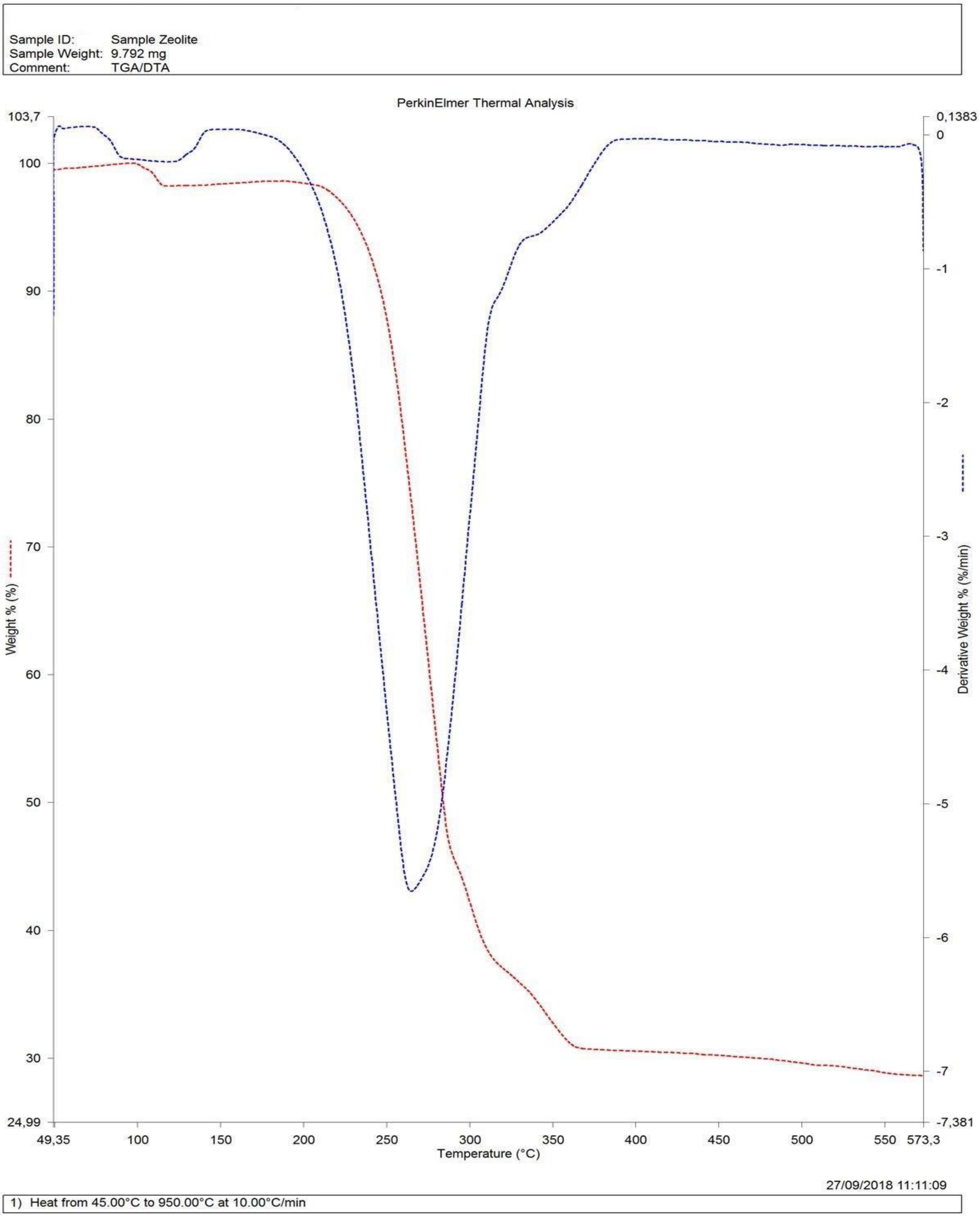

Figure 4.1b: TGA/DTA before adsorption (Zeolite)

4.1.2 Fourier transform infrared spectroscopy (FTIR)

The FTIR spectra for the samples are shown in Fgure 4.2a and 4.2b represent the file spectra of activated carbon and zeolite respectively. From Figure 4.2a, the peaks from 3853 to 3447.03 cm^{-1} correspond to O-H stretching bands of N.H groups, the peaks at 1636.34 cm^{-1} are assigned to type -1 and 11amide. The peak at 1399.34 cm^{-1} and 799.64 cm^{-1}, assigned to as systematical and root of plane stretching CO^2_3 peak at 1100.85 cm^{-1} correspond to P-O stretches in PO^3_4. (Mondal *et al.*, 2016). Peaks at 549.15 cm^{-1} relate to the different of stretches of the P-O bond in $PO^{2-}_{4.}$

From Figure 4.2b, the peaks measured were the range of 4000 to 500 cm^{-1}. The analysis showed the presence of the following 3448.39 cm^{-1} correspond to O-H stretching, the peak at 2923.18 cm^{-1} correspond to C-H stretching belonging to carbon skeleton. Also peak exhibited at 1628.09 cm^{-1} correspond to C=C or asymmetric and symmetric stretching C=O vibration (Alhassan *et al*, 2016). The peaks observed from both adsorbents shows the following similarities in the O-H stretching corresponding to 3853.42 to 3448.39 cm^{-1}, peaks at 1628.009 to 1399.34 cm^{-1} the presence alkyl halids, alkenes, nitrogen compounds secondary and tertiary amides.

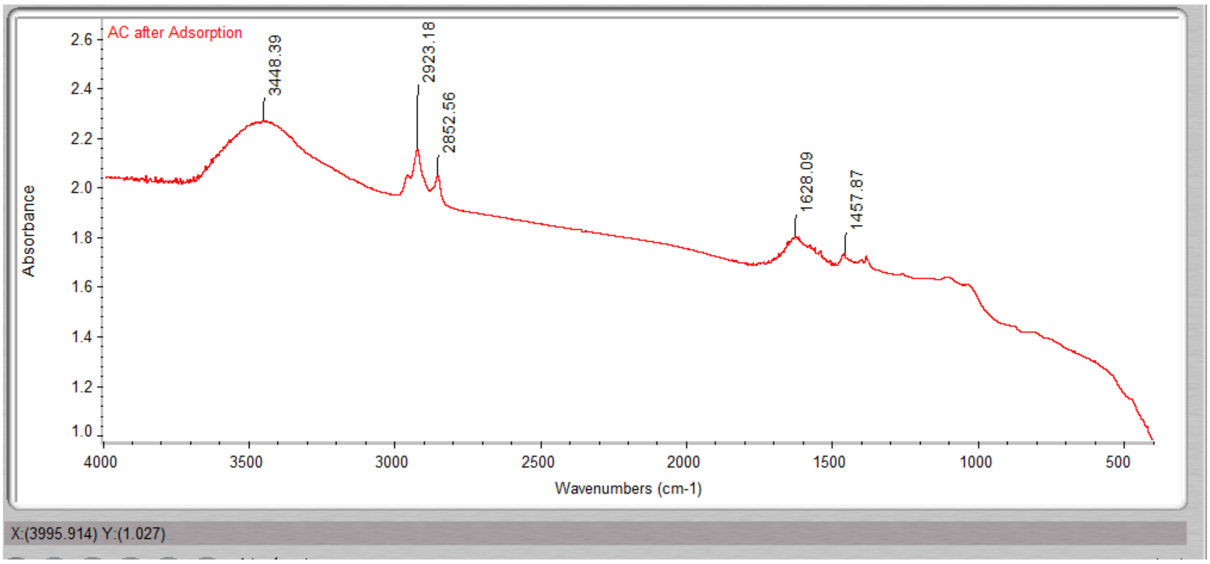

Figure 4.2 a: FT-IR spectra for activated carbon

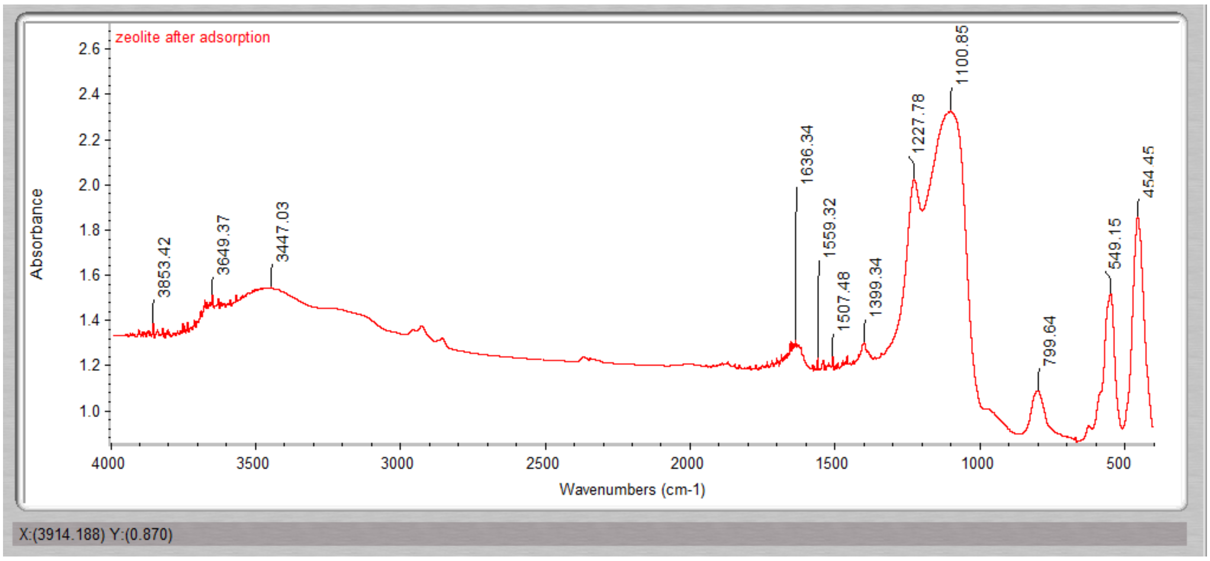

Figure 4.2 b: FT-IR spectra for zeolite

4.1.3 Scanning electron microscopy (SEM)

SEM was used, to observe the surface morphology of the adsorbents, (activated carbon and zeolite), before and after adsorption. These are show in Figure 4.3a – 4.3d.

Figure 4.3a show the morphological structure of activated carbon before adsorption with a well-developed pore structure of a regular average dimensions, while the Figure 4.3b shows a less regular dimension due to the co_2 adsorbed on the surface. Also figure 4.3c and 4.3d represent, the morphological structure of zeolite before and after adsorption. Figure 4.3c shows a numerous pores on co_2 could be adsorbed, while in figure 4.3d, most of the pores were covered. The SEM shows that the morphological structure of AC is well developed than that of zeolite, this also account for the high adsorption capacity using AC.

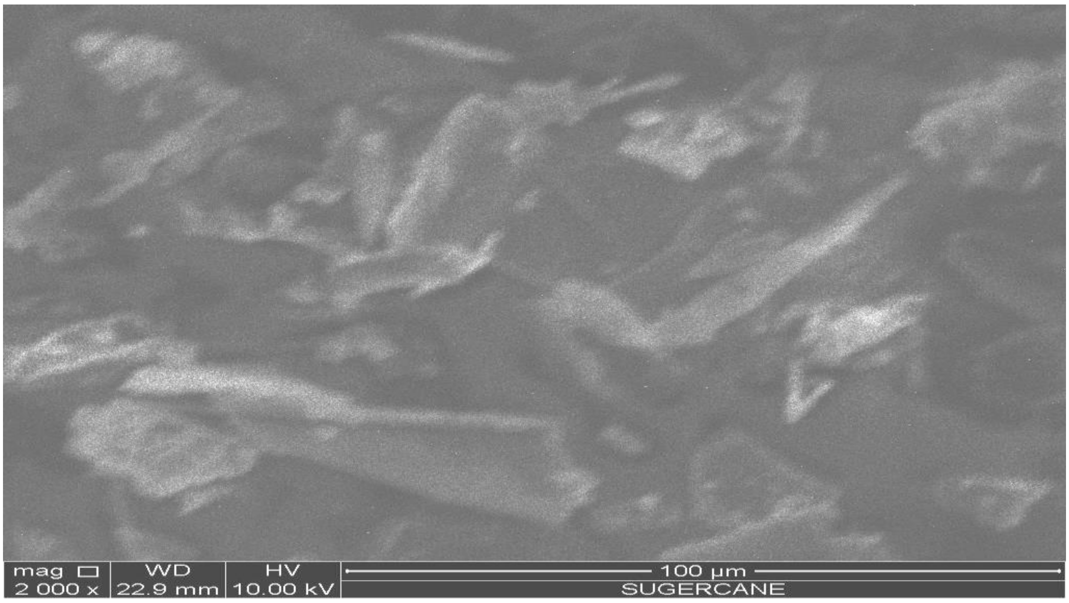

Figure 4.3 a: SEM for activated carbon before adsorption

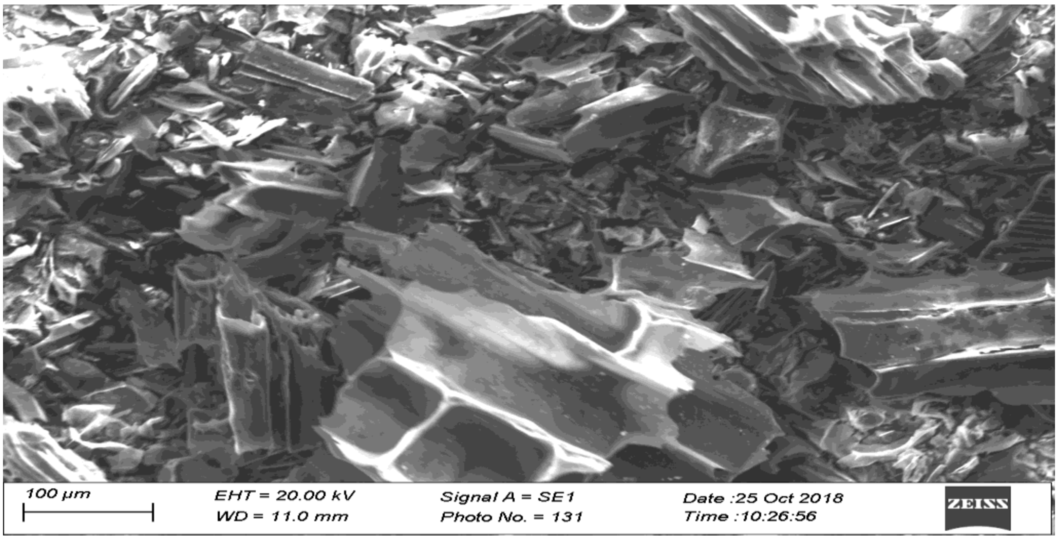

Figure 4.3 b: SEM for activated carbon after adsorption

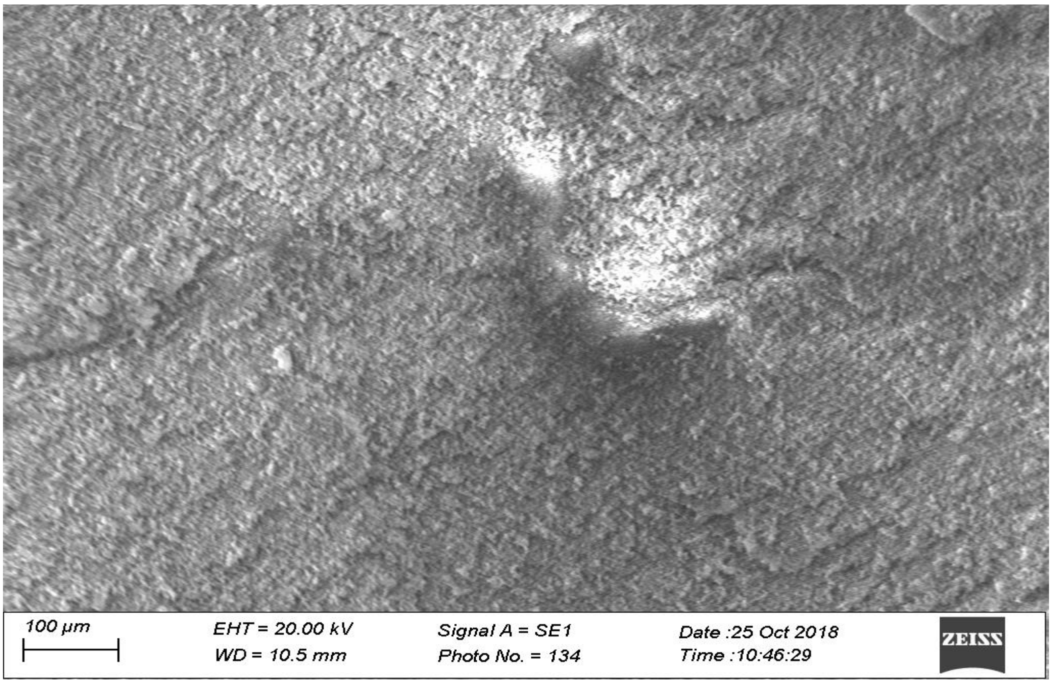

Figure 4.3 c: SEM for zeolite after adsorption

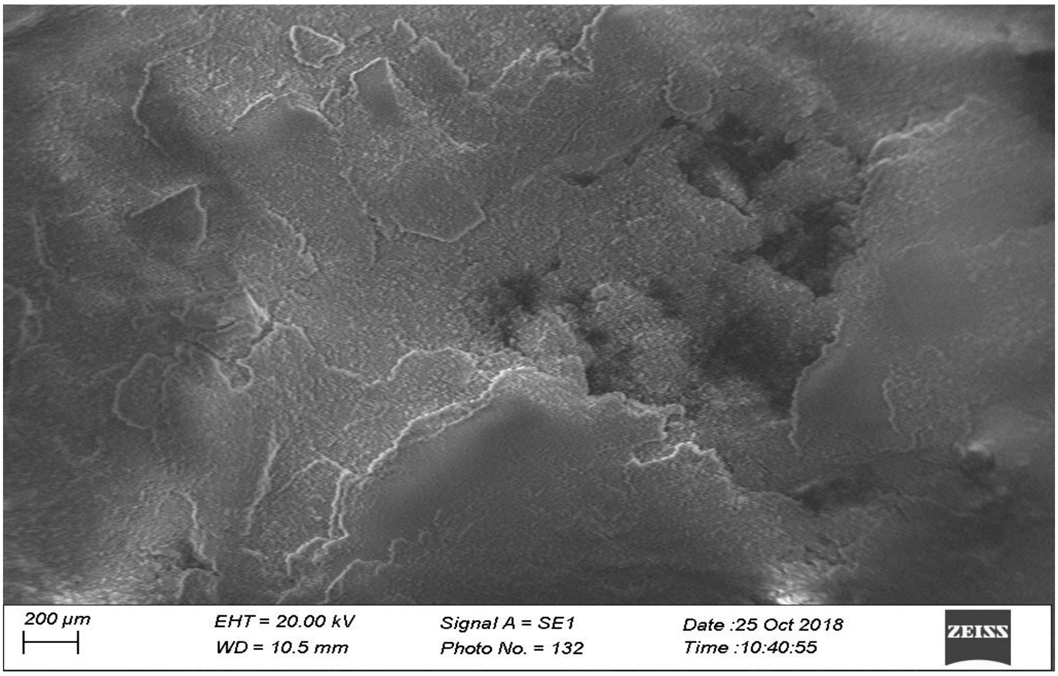

Figure 4.3 d: SEM for zeolite before adsorption

4.1.4 Brunauer-emmett-teller (BET) analysis

The BET analysis for activated carbon and zeolite was investigated to know the surface area, pore size and pore volume of the adsorbents. The result are shown in Table 4.1, the surface area of zeolite (388.2m^2/g) was greater than 224.2m^2/g of activated carbon, as a result of this one would expect zeolite to capture more CO_2 than activated carbon, this is no true because, the average pore size of activated carbon (5.878nm) is greater than 4.009nm of zeolite. Thus both surface and internal adsorption takes place using activated carbon, whereas only surface adsorption takes place using zeolite, because the average pore size of CO_2 is 3.73nm.

Table 4.1: BET result for the adsorbents

	Activated carbon	**Zeolite**
Properties	**Values**	**Values**
BET surface area (m^2/g)	224.2	388.2
Pore volume (cc/g)	0.1363	0.2131
Average pore size (nm)	5.878	4.009

4.2 Effect of adsorbent dosage

Effect of adsorbent dosage or bed height 2.7, 5.4 and 8.1 cm which are equivalent to 0.5, 1 and 1.5g respectively of adsorbent were used and the amount of CO_2 adsorbed at different time interval of 10 to 60 mins were determined at a constant flow rate of 1L/mins using activated carbon and zeolite from figure 4.2 a and 4.2 b, it is seen that an increase in the adsorbent dosage increase the adsorption capacities of the adsorbent. For 0.5 and 1g of Activated carbon, 57.2 and 60 mg/g of CO_2 was absorbed respectively, and for 0.5 and 1g of zeolite, 47.8 and 49 mg/g of CO_2 was absorbed respectively. The increase in the amount of CO_2 is due to the increase in the active side of the absorbent. The amount of CO_2 adsorbed at 1.5g of activated carbon and zeolite which are 65 and 50 mg/g respectively recorded, are the highest capacity obtained. The observation shows appreciable consistency with the report of (Alhasasan *et al.,* 2017)

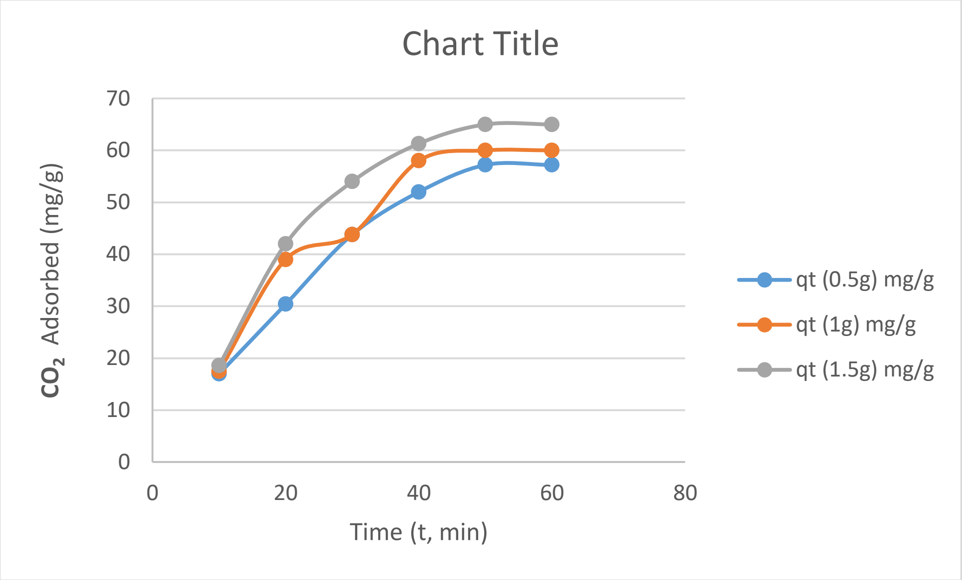

Figure 4.4a: Effect of adsorbent dosage using zeolite activated carbon

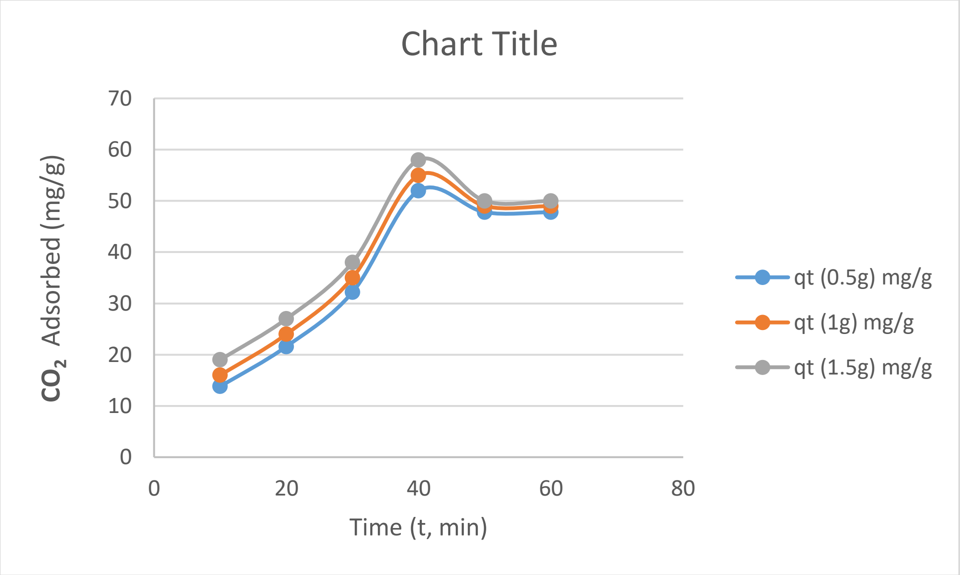

Figure 4.4b: Effect of adsorbent dosage using zeolite

From Figure 4.2a and Figure 4.2b, an increase in the adsorbent dosage increases the adsorption capacities of the adsorbents, this is because the diffusion of CO_2 through the pores of the adsorbent is limited due to compartment as the bed height is increased (Zulkurnai *et al*., 2013), and also takes longer time to attain saturation (Alhassan *et al*., 2016)

4.3 Effect of Temperature

The adsorption study was tested under the temperature range between 25-100^{O}C. The adsorption capacities were observed to be decreasing from 65 to 61.87 mg/g and from 50 to 47.67 mg/g for activated carbon and zeolite respectively, as temperature increase from 25^{O}C to 100^{O}C using both activated carbon and zeolite. This is a particular phenomenon in physisorption.

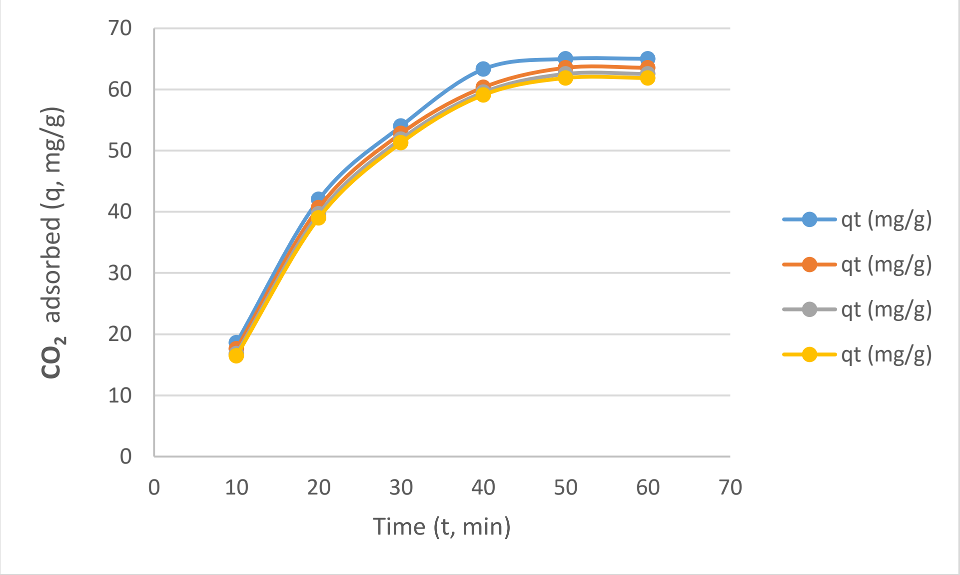

Figure 4.5 a: Effect of temperature using activated carbon

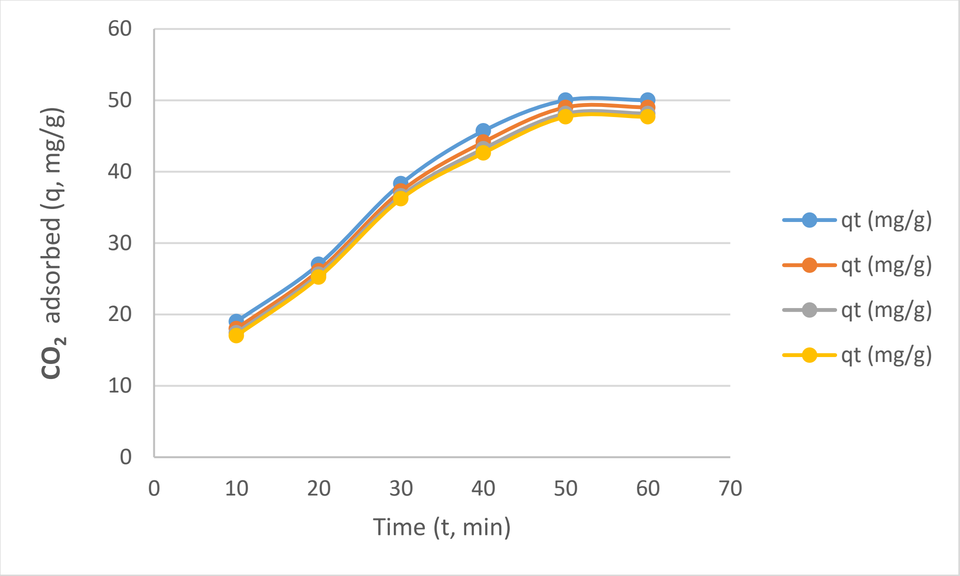

Figure 4.5 b: Effect of temperature using zeolite

From Figure 4.3a and 4.3b, the decrease in adsorption capacities as a result of an increase in temperature is due the reduction in the binding strength between the adsorbate and the adsorbents (Singh and Kurma, 2015). The decrease in adsorption capacities indicate, that the adsorption process is exothermic, (physical adsorption), (Rashidi *et al*., 2013). Also the breaken of the Van dar Waal forces is responsible for physisorption (Alhassan *et al*., 2016).

4.4 CO_2 Adsorption Isotherms

The adsorption process can be described with the Langmuir, Freundlich and Temkin models (Senthilkumaar *et al*., 2005), for the two adsorbents used in the adsorption process. In this study, the isotherm models were studied to describe the relationship between the level of adsorption and the adsorbent. From Table 4.2, using activated carbon and varying temperatures from 25 to 100^{O}C, the amount of the correlation coefficient [R^2] shows the Langmuir and Temkin models fitted well into the experimental data with R^2 values of 0.9675 and 0.9685 respectively, which are slightly higher than that of Freundlich model with R^2 values of 0.9085.

Table 4.2 Adsorption Isotherm parameters for activated carbon

Isotherm model	Parameters	Temperature (^{O}C)			
		25	50	75	100
Langmuir	Q_m (mgh/g)	222.2	238.1	270.3	277.8
	K_L (mol/mg)	$9.53x10^{-3}$	$833x10^{-3}$	$6.94x10^{-3}$	$6.59x10^{-3}$
	R^2	0.9675	0.9666	0.9648	0.9646
Frendlich	K_f	4.364	4.015	3.701	3.5785
	$\frac{1}{n}$	0.7014	0.716	0.733	0.7395
	R^2	0.908	0.9085	0.9072	0.9078
Temkin	K_t	0.5159	0.5218	0.5282	0.5308
	B	41.059	41.074	41.746	41.854
	R^2	0.96311	0.9685	0.968	0.9678

From Table 4.3, the adsorption experimental data using zeolite as an adsorbent, fitted well on all the three models. The R^2 values recorded for Langmuir, Freundich and Temkin are 0.9859, 0.9767 and 0.9744 respectively with their corresponding temperatures of 100, 25 and 100^{O}C for Langmuir, Freundlich and Temkin respectively. The result of this studies shows significant corresponding with those of Alhassan *et al.,* (2017). The temperature values where the R^2 values where recorded high for Langmuir freundlich and Temkin models using are activated carbon 25, 50 and 50^{O}C respectively.

Table 4.3. Adsorption Isotherm parameter for zeolite

Isotherm model	Parameters	Temperature (^{O}C)			
		25	50	75	100
Langmuir	q_m (mgh/g)	77.51	78.74	79.365	79.365
	K_L (mol/mg)	0.0315	0.0288	0.0275	0.0267
	R^2	0.9788	0.9828	0.9848	0.9859
Freundlich	K_f	4.966	4.5373	4.3192	4.1553
	$\frac{1}{n}$	0.5843	0.646	0.6096	0.617
	R^2	0.9767	0.979	0.9794	0.9796
Temkin	K_t	0.4886	0.4999	0.5043	0.5085
	B	26.718	27.459	27.457	27.758
	R^2	0.9696	0.9725	0.9739	0.9744

From Table 4.2 and 4.3, the K_L, K_F and K_T which are the Langmuir, Freundlich and Temkin rate constants respectively, indicates the adsorption capacity. K_L and K_F decreases with an increase in temperature, whereas K_T increases with increases in temperature. This result shows appreciable agreement with Wei *et al* (2015). The values of 1/n which ranges from 0.1-1.0, indicates favorable adsorption process (Wei *et al*., 2015).

4.5 CO_2 Adsorption Kinetic

Adsorption kinetic signifies the rate of molecular uptake from the adsorbate surface after overcoming the intermolecular and intramolecular forces impeding the adsorption process (Somasundaran *et al*., 1998, Kent, 2003). The kinetic models used to test the experimental data include pseudo first order kinetic, pseudo second order kinetic and intra particle diffusion models using activated carbon and zeolite as adsorbents. Table 4.4 shows the kinetic parameters obtained from the study using activated carbon adsorbent. From Table

4.4, the experimental data fitted well on the pseudo first order and intra particle diffusion kinetic models with R^2 values of 0.966 and 0.909 respectively. The R^2 value recorded for pseudo second order models is 0.8265 at corresponding temperature of 50^OC.

Table 4.4: Kinetic parameters on CO_2 Adsorption using AC

Kinetic model	**Parameters**	**Temperature (^OC)**			
		25	50	75	100
Psuedo first Order	K_1 (min^{-1})	0.0871	0.08498	0.085	0.0852
	q_e (mglg)	109.5	114.3	111.4	110.2
	R^2	0.9303	0.966	0.9644	0.9618
Psuedo second order	K_2(g/mg.min$^{-1)}$	1.864×10^{-4}	1.7483×10^{-4}	1.5814×10^{-4}	1.545×10^{-4}
	q_e(mg/g)	121.95	122	125	125
	R^2	0.8242	0.8265	0.7963	0.7856
Intra particle Diffusion	K(mg/g.min^{-1})	10.248	10.085	10.057	10.008
	C	7.186	7.8287	8.5914	8.8731
	R^2	0.9021	0.909	0.9085	0.9086

From Table 4.4, the CO_2 adsorption capacity of 125mg/g and 114.3mg/g were obtained from pseudo second order and pseudo first order respectively. This result shows slight conformity with the result of Alhassan *et al* (2017).

From Table 4.5, all the kinetic models fitted into the experimental data using zeolite adsorbent. The R^2 values of 0.9473, 0.9633 and 0.9691 were recorded for pseudo first order, pseudo second order and intra particle diffusion models respectively at a corresponding temperature of 25, 75 and 100^{O}C.

Table 4.5: Kinetic parameters on CO_2 adsorption using Zeolite

Kinetic model	**Parameters**	**Temperature (^{O}C)**			
		25	50	75	100
Psued first Order	K_1 (min^{-1})	0.07876	0.0783	0.0781	0.0778
	q_e (mg/g)	90.53	91.12	89.62	89.43
	R^2	0.9473	0.9436	0.9436	0.9425
Psued second order	K_2(g/mg.min$^{-1)}$	3.4×10^{-4}	3.14×10^{-4}	3.092×10^{-4}	3.011×10^{-4}
	q_e(mg/g)	82.65	83.33	82.6	82.6
	R^2	0.9622	0.963	0.9633	0.9623
Intra particle Diffusion	K(mg/g.min^{-1})	7.4347	7.3997	7.3173	7.2977
	C	4.1104	4.9893	5.2637	5.5878
	R^2	0.964	0.9679	0.9685	0.9691

In Table 4.5, the CO_2 adsorption capacity of 91.12 and 83.33mg/g were obtained from pseudo first order and pseudo second order models respectively. This result shows slight conformity with the result of Alhassan *et al.,* (2017).

From Table 4.4 and 4.5, the values of first order (K_1) and second order (K_2) rate constant decreases as temperature increases. Also the values of the correlation coefficient R^2, closeness to unity indicates that the experimental data validates the kinetic models tested (Lim *et al.*, 2009).

4.6 Activation Energy

According to Alhassan *et al*. (2017), activation energy gives an insight information on the adsorption mechanism and its magnitude indicate whether the adsorption process is physisorption (E_a = 5 – 40 KJ/mol) or chemisorption (E_a = 40 – 800 KJ/mol). In this report, the activation energy obtained using activated carbon and zeolite are 15.3 and 13.5 KJ/mol, which signifies that the adsorption process is physisorption. The activation energy obtained in this report falls within the range of most adsorption process using similar adsorbents as reported by Alhassan *et al*. (2016).

CHAPTER FIVE

5.0 CONCLUSION AND RECOMMENDATION

5.1 Conclusion

The result from the characterization of the activated carbon produced and zeolite purchased, revealed a better surface morphology for the both adsorbents using SEM. The BET analysis investigated on the adsorbent shows, a surface area of 224.2 m^2/g and an average pore size of 5.878 nm for activated carbon and surface area of 388.2 m^2/g and average pore size of 4.009 nm for zeolite. The FT-IR analysis for activated carbon zeolite revealed the presence of hydroxyl and carboxylic stretch bands. The CO_2 adsorption capacity shows an increase in the adsorbent dosage from 0.5g to 1.5g while an increase in temperature from 25 to 100^OC, shows a decreasing trend in the CO_2 adsorption capacity. The adsorption capacity of the adsorbents were determined and the result revealed that the amount of CO_2 adsorbed using activated carbon (65 mg/g) was higher than that of the zeolite (50 mg/g), however for both adsorbents, the adsorption capacity were higher than that of the commercial adsorbents when compared. The adsorption isotherm models used in testing the adsorption experimental data are Langmuir, Freundlich and Temkin Isotherm. The data use from the activated carbon fitted well into Langmuir and Temkin models with correlation coefficient R^2 values of 0.9675 and 0.9685 respectively. These data, also fitted well on the three isotherm models using zeolite with R^2 values 0.9859, 0.9767 and 0.9744 for Langmuir, Freundlich and Temkin Isotherm models respectively. The adsorption kinetic study shows that the adsorption data fitted well on pseudo first order and intra particles diffusion models using activated carbon as adsorbent with R^2 values of 0.966 and 0.909 respectively. The activation energy E_a of 15.3 and 13.5KJ/mol for activated carbon and zeolite obeys physiosorption.

Activated carbon and zeolite were found to good adsorbent for CO_2 removal, the CO_2 adsorption capacities were greater in activated carbon (65 mg/g) than zeolite (50 mg/g), as a result of its high porosity and surface area that allow both surface and internal adsorption of CO_2.

5.2 Recommendations

The increase in energy demand and the use of non-renewable fossil fuels to meet the energy demand globally, will continue to increase CO_2 emission to the atmosphere hence that is need for the removal or adsorption of these excess CO_2 from the atmosphere. A lot of another have reported the use of activated carbon and zeolite as good adsorbent for CO_2 capture, therefore my recommendation goes thus.

1. Zeolite and activated carbon should be marshal together and used as adsorbent for excess CO_2 removal from the atmosphere and the adsorption capacity from the meshed adsorbent be compared to that of the individual adsorbent zeolite and activated carbon.
2. A thermo-gravimetric analyzer should be used instead of a batch adsorption column due to the difficultly in measurement using the analytical weighing balance.

REFERENCES

Abia, A. A. & Igwe, J. C. (2005). "Sorption kinetics and intraparticle diffusivities of Cd,

Pd and Zn ions on maize cob", African Journal of Biotechnology, 4, 6, 509-512.

Adilla, N., Yusup, S., & Hameed, B. H. (2013). Kinetic studies on carbon dioxide capture using lignocellulosic based activated carbon. *Energy*, 1–7. https://doi.org/10.1016/j.energy.2013.08.050

Alhassan, M., Auta, M., Sabo, J. K., Umaru, M., Garba, M. U., & Kovo, A. S. (2016). CO_2 capture using Amine-impregnated activated carbon from Jatropha curcas shell, 14(4), 1-11 https://doi.org/10.9734/BJAST/24253

Alhassan, M., Andrew, I., Auta, M., Umaru, M., Garba, M. U., & Isa, A. G. (2017). Comparative Studies of CO_2 capture using acid and base modified activated carbon from sugar cane bagasse. Biofuels, https://doi.org/10.1080/17597269.1306680

AlOthman, Z., Habila, M., & Ali, R. (2011). Preparation of Activated Carbon Using the Copyrolysis of Agricultural and Municipal Solid Wastes at a Low Carbonization Temperature. *Carbon*, *24*, 67–72. https://doi.org/10.13140/2.1.1478.2401

Aranovich, G. & Donohue, M. (1998). Analysis of Adsorption Isotherms: Lattice Theory Predictions, Classification of Isotherms for Gas–Solid Equilibria, and Similarities in Gas and Liquid Adsorption Behavior. *Journal Colloid Interface Science*, 20(10), pp. 273–290

Bansal, R.C. & M. Goyal, (2005). Activated Carbon Adsorption. Boca Raton, FL: CRC Press.

Bansode, R. R., Losso, J. N., Marshall, W. E., Rao, R.M. & Portier, R. J. (2003). Adsorption of Volatile Organic Compounds by Pecan Shell and Almond Shell Based Granular Activated Carbons. Journal of Bioresource Technology, 90(12), pp. 175-184.

Beguin, F. & Frackowiak, E. (2010). Carbons for Electrochemical Energy Storage and Conversion Systems. CRC Press.

Bhatt, A. G. & R. (2012). Causes and Concequences of Global Warming. *Indian Journal of Life Sciences Biotechnology and Pharma Research*, *1*(1), 27–31.

Bhattacharjee, P. K. (2010). Global Warming Impact on the Earth. *International Journal of Environmental Science and Development*, *1*(3), 219–220.

Bilal, A., Akash, W. & O'Brien, (1996). The Production of Activated Carbon from a Bituminous Coal,*International Journal of Energy Resources*, 20(10), pp. 913.

Chaffee, A. L., Knowles, G. P., Liang, Z., Zhang, J., Xiao, P., & Webley, P. A. (2007). CO_2 capture by adsorption : Materials and process development. *International Journal of Greenhouse Gas Control*, *1*, 11–18. https://doi.org/10.1016/S1750-5836(07)00031-X

Chandel, A. K., Silva, S., & Singh, O. V. (2012). Sugarcane bagasse and leaves : foreseeable biomass of biofuel and bio-products. *Journal of ChemicalnTechnology and Biotechnology*, *87*, 11–20. https://doi.org/10.1002/jctb.2742

Coulson, J. M., & Richardson, J. F. (1991). *Particle Technology and Separation Processes*. *Chemical Engineering* (fifth, Vol. 2). Oxford: Btterworth-Heinemann.

Creamer, A. E., Gao, B., & Zhang, M. (2014). Carbon dioxide capture using biochar produced from sugarcane bagasse and hickory wood. *Chemical Engineering Journal*, *249*, 174–179. https://doi.org/10.1016/j.cej.2014.03.105

Danielle, B., Mourad, K., Patrick, N., Murielle, M., & Robert, H., (2008) Advances in principal factors influencing carbon dioxide adsorption on zeolites. *Sci. Technol. Adv. Mater*.9, 1-7. doi:10.1088/1468-6996/9/1/013007

Daud, W., Ali, W. & Suleiman, M. Z. (2000). The effects of carbonization temperature on pore development in palm-shell-based activated carbon, Carbon Journal 38 (24), pp. 1925-1932.

David, E., & Kopac, J. (2014). Activated carbons derived from residual biomass pyrolysis and their CO_2 adsorption capacity. *Journal of Analytical and Applied Pyrolysis*, *110*(1), 322–332. https://doi.org/10.1016/j.jaap.2014.09.021

Dhillon, R. S., & Wuehlisch, G. Von. (2013). Mitigation of global warming through renewable biomass. *Biomass and Bioenergy*, *48*, 75–89. https://doi.org/10.1016/j.biombioe.2012.11.005

Dqbrowski, A. (2001). Adsorption from theory to practice. *Elsevier*, *93*, 135–224.

Ferrari, L., Kaufmann, J., Winnefeld, F., & Plank, J. (2010). Interaction of cement model systems with superplasticizers investigated by atomic force microscopy, zeta potential, and adsorption measurements. *Journal of Colloid and Interface Science*, *347*(1), 15–24. https://doi.org/10.1016/j.jcis.2010.03.005

Foo, K. Y., & Hameed, B. H. (2010). Insights into the modeling of adsorption isotherm systems. *Elsevier*, *156*, 2–10. https://doi.org/10.1016/j.cej.2009.09.013

Gupta, V. K., Mittal, A. L., Krishnan L., Mittal, J. & Coll, J. (2005). Journal Interface Science, 29(3), 16-21.

Han, Y. W., Catalano, E. A., & Ciegler, A. (1983). Chemical and Physical Properties of Sugarcane Bagasse Irradiated with Gamma Rays. *Journal of Agriculture and Food Chemistry*, *31*(1), 34–38.

Hileman B., (2006) Climate change threatens global economy, *Chemical & Engineering News*, *84*, *7–8.*

Hsia, D. S. (2014). *Potential Health Benefits of a Natural Fiber from Sugarcane*. *Pennington Biomedical*. Louisiana. Retrieved from www.pbrc.edu

Ifechukwu G. Ezemagu, Mathew C. Menkiti, V. I. U. & M. C. A. (2016). Adsorptive Approach on Nepholometric Study of Paint Effluent Using Tympanotonos Fuscatus Extract. *Chemical Society of Ethiopia*, *30*(3), 377–390. https://doi.org/http://dx.doi.org/10.4314/bcse.v30i3.6

Incoporated, C. (2006). ACTIVATED CARBON.

IPCC, & Press, C. U. (2013). Climate Change 2013: The Physical Science Basis. *Climate Change 2013*, (September 2013), 1535. https://doi.org/10.1017/CBO9781107415324

Jabit, N. B. (2007). *The Production And Characterization Of Activated Carbon Using Local Agricultural*. Retrieved from http://eprints.usm.my/9576/1/

Jacoby, J. P. C. & L. S. (2014). The challenges of global warming research. In *Crime, Violence and Global Warming* (pp. 3–21). https://doi.org/10.1016/B978-0-323-26509-6.00001-2

Jacoby, J. P. C. & L. S. (2015). What is Global Warming. In *Crime, Violence and Global Warming* (pp. 23–50). Taylor & Francis. https://doi.org/10.1016/B978-0-323-26509-6.00002-4

Jankowska, H., Swiatkowski, A. and Chioma, J. (1991). *Active Carbon*. Ellis Horwood Limited.

Jian-bin, H., Shao-wu, W., Yong, L. U. O., Zong-ci, Z., & Xin-yu, W. E. N. (2012). Debates on the Causes of Global Warming. *Advances in Climate Change Research*, *3*(1), 38–44. https://doi.org/10.3724/SP.J.1248.2012.00038

Kadirvelu, K., Karthika, C., Vennilamani, N. & Pattabhi, S. (2005). Chemosphere Journal, 60, pp. 1009.

Kannan, N. & Pagutharivalan, R. (2012). Removal of Basic Green Dye from Aqueous Media by using Eucalyptus Globules Cark carbon as an Adsorbent-A comparative study. Journal Chemical Pharma Resource 4(1), pp. 38–45.

Kent, S. K. (2003). “Adsorbent Selection”, Adsorption Research, Inc., Dublin, Ohio, 43016, 1-23.

Kim, M., & Day, D. F. (2011). Composition of sugar cane , energy cane , and sweet sorghum suitable for ethanol production at Louisiana sugar mills. *Journal of Industrial Microbiol Biotechnol*, *38*, 803–807. https://doi.org/10.1007/s10295-010-0812-8

Kirk-Othmer. (2014). Activated carbon 1.

Kralik, M. (2014). REVIEW Adsorption, chemisorption, and catalysis. *Versita*, *68*(12), 1625–1638. https://doi.org/10.2478/s11696-014-0624-9

Kumar S., H. S. K. & G. K. K. (2014). Effect of Global Warming on Mankind -A Review Effect of Global Warming on Mankind - A Review. *International Research Journal of Environmental Science*, *1*(14), 56–59.

Leimkuehler, E. P., Suppes, G. J., & Supervisor, T. (2010). Production, Characterization, and Applications of Activated Carbon. *Article*, (May), 11. Retrieved from https://mospace.umsystem.edu/xmlui/bitstream/handle/10355/8078/research.pdf?sequence=

Lim, K., Pan, J., Chen, Y., Cheng, R., & Xu, X. (2009). “Study the adsorption of phenol from aqueous solution on hydroxyapatite nano powders”. J Hazard Mater. 161(1), 231-240.

Lua, A. C., & Guo, J. (2001). Microporous oil-palm-shell activated carbon prepared by physical activation for gas-phase adsorption. *Langmuir*, *17*(22), 7112–7117. https://doi.org/10.1021/la010290c

Lua, C. & Guo J. (2001). Preparation and characterization of activated carbons from oil-palm stones for gas-phase adsorption,” *Colloids Surf. A*, 179, 151-162.

Mendez, M.O.A., Lisboa, A.C.L., Coutinhoand, A.R. & Otani, C. (2006). Activated Petroleum Coke for natural gas storage. Journal of Brazil Chemical Society, 17(6), pp. 1144-1150.

Michael, M., Brittain, M. & Nagai, J. (2004). Phase II Study of Activated Charcoal to Prevent Irinotecan Induced Diarrhea, Journal of Clinical Oncology, 22 (21), pp.4–7.

Molina-Sabio, M., Gonzalez, M. T., Rodriguez-Reinoso, F. & Sepulveda-Escribano, A. (1996). Effect of Steam and Carbon Dioxide Activation in the Micro Pore Size Distribution of Activated Carbon. *Carbon Journal* 34(4), pp. 505–509

Nakagawa, K., Mukai, S. R., Suzuki, T. & Tamon, H. (2003). Gas Adsorption on Activated Carbons from PET Mixtures with a Metal Salt, Carbon Journal 41(23), pp. 823-831.

Namasivayam, C., Kumar, M. D., Kumar, S., Begum, R. A., Vanathi, T. & Yamuna, R. T. (2005). Journal of Biomass Bioenergy, 21(8), pp. 477.

Ozacar M., & Sengil, A. I. (2005). Journal of Bioresource Technology, 9(6), pp. 791.

Paiva, S. L. D., Savi, M. A., Viola, F. M., & Leiroz, A. J. K. (2014). BioSystems Global warming description using Daisyworld model with greenhouse gases. *BioSystems*, *125*, 1–15. https://doi.org/10.1016/j.biosystems.2014.09.008

Pereira, P. H. F., Jacobus, C., Cioffi, M. O. H., Mulinari, R., & Luz, M. Da. (2011). Sugarcane bagasse pulping and bleaching: thermal and chemical characterization. *Bioresources.com*, *6*(3), 2471–2482.

Plaza M. G., Pevida, C., Arenillas, A., Rubiera, F. & Pis, J. J. (2012). CO_2 capture by adsorption with nitrogen enriched carbons," *Fuel*, 86, 2204-2212.

Purba E., & Taharuddin T., (2010) CO_2 reduction and production of algal oil using microalgae nannochloro psisoculata and tetra selmischuii, *Chemical Engineering Transactions, 21, 397-402, DOI: 10.3303/CET1021067.*

Puziy, A. M., Poddubnaya O. I., Matinez-Alonso, A. Suarez-Garcia, F. & Tascon, J. M. D. (2006). Characterization of Synthetic Carbon Activated with Phosphoric Acid, Journal of Applied Surface Science, 20(10), pp. 196-202.

Rajeshwarisivaraj, R., Sivakumar, S., Senthilkumar, P. & Subburam, V. (2001). Carbon from Cassava Peel, an Agricultural Waste, as an Adsorbent in the Removal of Dyes and Metal Ions from Aqueous Solutions. Journal of Bioresource Technology 80(32), pp. 233–235.

Rashidi, N. A., Yusup, S., & Lam, H. L. (2013). Kinetic studies on carbon dioxide capture using lignocellulosic based activated carbon, Energy 61. 440-446.

Rashidi, N. A., Yusup, S. & Borhan A. (2014). Development of Novel Low-Cost Activated Carbon for Carbon Dioxide Capture. *International Journal of Chemical Engineering and Applications,*5(2), 1-5.

Rengarag, S., Seung-Hyeon M., Sivabalan S., Arabindoo, B. & Murugesan, V. (2002). Agricultural Solid Waste for the Removal of Organics: Adsorption of Phenol from Water and Wastewater by Palm Seed Coat Activated Carbon. *Waste Management Journal* 2(22), pp. 543-548

Rodriguez-Reinoso, F., Molina-Sabio, M. & Gonzalez, M. T. (1995). The Use of Steam and CO_2 as Activating Agents in the Preparation of Activated Carbons comparison of isotherm models, *Bioresource Technology Journal*, 98(21), pp. 1812-1821.

Rudolph, V., Rasul, M. G., Rudolph, V., & Carsky, M. (1999). Physical properties of bagasse. *Fuel*, *78*, 905–910. https://doi.org/10.1016/S0016-2361(99)00011-3

Somansundaran, P., Shrotri, S., & Huang, L. (1998). "Thermodynamics of Adsorption of Surfactant at soli-liquid interface", Pure and Appl. Chem, 70. 3. 621-626.

Senthilkumar, S., Varadarajan, P. R., Porkodi, K. & Subbhuraam, C.V. (2005). Adsorption of Methylene Blue onto Jute Fiber Carbon: Kinetics and Equilibrium Studies. Journal Colloid Interface Science, 28(4), pp. 78–82.

Senthilkurmaar, S., Varadarajan, P. R., Porkodi, K., & Subbhuraam, J. (2005). Colloid Interface Sci. **284**, 722.

Shah, parag S. (2007). *Nanoporous carbon from corn cobs and its application*. university of Missouri- Columbia.

Silvestre-Albero, F. R.-R. & J. (2016). Activated Carbon and Adsorption. *Carbon*, 1–14. https://doi.org/10.1016/B978-0-12-803581-8.02289-X

Singh, V. K., & Kumar, E. A. (2015). Comparative Studies on CO_2 Adsorption Kinetics by Solid Adsorbents. In *Energy Procedia* (Vol. 90, pp. 316–325). The Author(s). https://doi.org/10.1016/j.egypro.2016.11.199

Sivakumar, B., Kannan, C. & Karthikeyan, S. (2012). Preparation and Characterization of Activated Carbon Prepared from Balsamodendron Caudatum Wood Waste through Various Activation Processes, Carbon Journal, 5(3), 321-327.

Smil, V. (2003). *The Earth's Biosphere: Evolution, Dynamics, and Change.* MIT Press.

Smisek M. & Cerney S. (1970). Active carbon: Manufacture, Properties and Applications, Carbon Journal, 21(32), pp. 1123-1127.

Solomon, S., D. Qin, M. Manning, Z. Chen, M. Marquis, K. B. A., & Miller, M. T. and H. L. (2007a). *The Physical Science Basis. Contribution of Working Group I to the Fourth Assessment Report of the Intergovernmental Panel on Climate Change*. *IPCC, 2007: Climate Change 2007*. Cambridge.

Solomon, S., D. Qin, M. Manning, Z. Chen, M. Marquis, K. B. A., & Miller, M. T. and H. L. (2007b). *The Physical Science Basis. Contribution of Working Group I to the Fourth Assessment Report of the Intergovernmental Panel on Climate Change*. Cambridge.

Sosa-Arnao, J. H., De Oliveira, F. M., Corrêa, J. L., Silva, M. A., & Nebra, S. A. (2004). Sugar Cane Bagasse Drying – a Review. *Drying 2004 – Proceedings of the 14th International Drying Symposium (IDS 2004)*, (March), 990–997.

Srinivasakannan, C. & Abu Baker M. Z. (2002). Production of Activated Carbon from Rubber Wood Sawdust. Journal of Biomass Bioenergy in press, 21(9), pp. 234-235.

Srinvaskannan, C. & Mohammad, Z. A. (2004). Production of Activated Carbon from Rubber Wood Sawdust. Biomass Bioenergy Journal. 27(6), pp. 89-96.

Sua´rez-Garcı´a, F., Martı´nez-Alonso, A., & Tascon, J. M. D. (2002). Pyrolysis of Apple Pulp: Chemical Activation with Phosphoric Acid, Journal Analytical Applied Pyrolysis 63(12), pp. 283-301.

Suhardy, D., Nasery, S., F. K. & S. S. (2005). Characterization Of Sugarcane Bagasse, Rice Straw And Rice Husk and their Suitability for Paper Production, 1–3.

Sutar, P. N., Jha, A., Vaidya, P. D., & Kenig, E. Y. (2012). Secondary amines for CO_2 capture : A kinetic investigation using N-ethylmonoethanolamine. *CHEMICAL ENGINEERING JOURNAL*. https://doi.org/10.1016/j.cej.2012.07.042

Sutrisno, B., Noni, A, Annisa, S. H. & Arif, H. (2016). Preparation and characterization of activated carbon from sugarcane bagasse by physical activation with CO_2 gas. *IOP Conf. Series: Materials Science and Engineering* 105 012027 doi:10.1088/1757-899X/105/1/012027.

Tan, I. A. W., Ahmad, A. L. & Hameed, B. H. (2008). Optimization of Preparation Conditions for Activated Carbons from Coconut Husk Using Response Surface Methodology. *Chemical Engineering Journal* 37(6), pp. 462–470.

Theivarasu, C., & Mylsamy, S. (2011). "Removal of Malachite Green from Aqueous Solution by Activated Carbon Developed from Cocoa (Theobroma Cacao) Shell—A Kinetic and Equilibrium Studies," EJournal of Chemistry, 8(1), pp. 363–371.

Thinakaran, N., Panneerselvam, P., Baskaralingam, P., Elango, D. & Sivanesan, S. (2008). Equilibrium and Kinetic Studies on the Removal of Acid Red 114 from Aqueous Solutions using Activated Carbons Prepared from Seed Shells. Journal Hazardous Material, 15(8), pp. 142–150.

Thomas, J.M. & Thomas, W.J. (1997). Principles and Practices of Heterogenous Catalysis. *Journal of Applied Surface Science*, 3(5), pp. 267-273.

Torregrosa-Macia, R., Martin-Martinez, J. M. & Mittelmeijer-Hazeleger, M. C. (1997). Porous Texture of Activated Carbons Modified with Carbohydrates. *Carbon Journal*, 35(4), pp. 447–453

Vasanth, K. & Sivanesan, S. (2005). Journals on Dyes Pigments, 7(2), pp. 124.

Venkataramanan, M. (2011). Causes and Effects of Global Warming. *Indian Journal of Science and Technology*, *4*(3), 3–6.

Walmsley, D. (2010). *Climate Change and its Effects On Humans, State of the Gulf of Maine Report*. Gulf of Maine.

Wei, W., Yang L., Zhongh, W. H., Li, S. Y., Cui, J., & Wei, Z. G. (2015). Fast Removal of Methylene Blue from Aqueous Solution by Adsorption onto poorly crystalline Hydroxyapatite Nanoparticles

Williams, P. T. & Reed, A. R. (2006). Development of Activated Carbon Pore Structure via Physical and Chemical Activation of Biomass Fibre Waste, Biomass and Bioenergy Journal, 30(15), pp.144-152.

Winter, R. A. (2014). Innovation and the dynamics of global warming. *Journal of Environmental Economics and Management*, *68*(1), 124–140. https://doi.org/10.1016/j.jeem.2014.01.005

Wu, X., Yu, Y., Qin, Z., & Zhang, Z. (2014). The advances of post-combustion CO_2 capture with chemical solvents: Review and guidelines. In *Energy Procedia* (Vol. 63, pp. 1339–1346). Elsevier B.V. https://doi.org/10.1016/j.egypro.2014.11.143

Yaumi, A. L., Bakar, M. Z. A., & Hameed, B. H. (2017). Recent advances in functionalized composite solid materials for carbon dioxide capture. *Energy*, *124*, 461–480. https://doi.org/10.1016/j.energy.2017.02.053

Yu, C., Huang, C., & Tan, C. (2012). A Review of CO_2 Capture by Absorption and Adsorption. *Aerosol and Air Quality Research, 12,* 745–769. https://doi.org/10.4209/aaqr.2012.05.0132

Zhang, X., Li, W., & Lu, A. (2015). Designed porous carbon materials for efficient CO_2 adsorption and separation. *New Carbon Materials*, *30*(6), 481–501. https://doi.org/10.1016/S1872-5805(15)60203-7.

Zulkurnai, N. Z., Ali, U. F., Ibrahim, N., & Abdul, N. S. (2018). Carbon Dioxide capture by Deep Eutectic Solvent Impregnated Sea Mango Activated Carbon http://doi.org/10.1051/e3sconf/20183402030.

APPENDIX A

Quantity of CO_2 adsorbed at 1 L/Min (Activated carbon)

Time (min)	CO_2 uptake (0.5g)mg	CO_2 uptake (1g)mg	CO_2 uptake (1.5g)mg	q_t (0.5g) mg/g	q_t (1g) mg/g	q_t (1.5g) mg/g
10	8.5	17.5	27.9	17	17.5	18.6
20	15.2	39.0	63.0	30.4	39.0	42.0
30	21.9	50.0	81.0	43.8	43.8	54.0
40	26.0	58.0	92.0	52.0	58.0	61.3
50	28.6	60.0	97.5	57.2	60.0	65.0
60	28.6	60.0	97.5	57.2	60.0	65.0

Quantity of CO_2 adsorbed at 1 L/Min (Zeolite)

Time (min)	CO_2 uptake (0.5g)mg	CO_2 uptake (1g)mg	CO_2 uptake (1.5g)mg	q_t (0.5g) mg/g	q_t (1g) mg/g	q_t (1.5g) mg/g
10	6.9	16.0	28.5	13.8	16.0	19.0
20	10.8	24.0	40.5	21.6	24.0	27.0
30	16.1	35.0	57.5	32.2	35.0	38.0
40	26.0	55.0	87.0	52.0	55.0	58.0
50	23.9	49.0	75.0	47.8	49.0	50.0
60	23.9	49.0	75.0	47.8	49.0	50.0

First order using activated carbon

Time (min)	**$q_e - q_e$ (mg/g) 25^{O}C**	**$q_e - q_t$ (mg/g) 50^{O}C**	**$q_e - q_t$ (mg/g) 75^{O}C**	**$q_e - q_t$ (mg/g) 100^{O}C**	**Log(q^e- q_t) 25^{O}C**	**Log(q_e– q_t) 50^{O}C**	**Log(q^e- q_t) 75^{O}C**	**Log(q_e^{-} q_t) 100^{O}C**
10	46.4	45.93	45.73	1.6665	1.6621	1.6621	1.66062	1.6571
20	23.0	22.86	22.86	22.87	1.3617	1.3591	1.3591	1.3593
30	11.0	10.73	10.66	10.6	1.0414	1.0306	1.0278	1.0253
40	1.7	3.2	3	2.77	0.2304	0.3051	0.4771	0.4425
50	0	0	0	0	0	0	0	0
60	0	0	0	0	0	0	0	0

q_e at 25^0c = 65.0mglg q_e at 50^0c =63.53

q_e at 75^0c = 62.53 q_e at 100^0c = 61.87

First order using zeolite

Time (min)	**$q_e - q_e$ (mg/g) 25^{O}C**	**$q_e - q_t$ (mg/g) 50^{O}C**	**$q_e - q_t$ (mg/g) 75^{O}C**	**$q_e - q_t$ (mg/g) 100^{O}C**	**Log(q^e- q_t) 25^{O}C**	**Log(q_e– q_t) 50^{O}C**	**Log(q^e- q_t) 75^{O}C**	**Log(q_e^{-} q_t) 100^{O}C**
10	31.0	31.0	30.73	1.49914	1.4914	1.4876	1.4876	1.4867
20	23.0	22.87	22.53	22.47	1.3617	1.3593	1.3528	1.3517
30	11.7	11.73	11.53	11.47	1.0693	1.0693	1.0618	1.0596
40	4.3	4.87	4.93	5.07	0.6335	0.6875	0.6928	0.7050
50	0	0	0	0	0	0	0	0
60	0	0	0	0	0	0	0	0

q_e at 25^0c = 50mg/g q_e at 50^0c = 49mg/g.

q_e at 75^0c = 48.13mg/g q_e at 100^0C= 47.64mg/g

Second order using activated carbon

Time (min)	q_e(mg/g) 25^0c	q_e(mg/g) 50^0c	q_e(mg/g) 75^0c	q_e(mg/g) 100^0c	t/q_e 25^0c	t/q_e 50^0c	t/q_e 75^0c	t/q_e 100^0c
10	18.6	17.6	16.8	16.7	0.5376	0.5662	0.5952	0.6077
20	42	40.67	39.67	39.0	0.9762	0.4918	0.5042	0.5128
30	54.0	52.8	51.87	51.27	0.5556	0.5682	0.5784	0.5851
40	63.3	60.33	59.53	59.10	0.6319	0.6630	0.6719	0.6768
50	65.0	63.53	62.53	61.87	0.7692	0.7870	0.7996	0.8081
60	65.0	63.53	62.53	61.87	0.9231	0.9444	0.9395	0.9698

Second order using zeolite

Time (min)	q_t(mg/g) 25^0c	q_t(mg/g) 50^0c	q_t(mg/g) 75^0c	q_t(mg/g) 100^0c	t/q_t 25^0c	t/q_t 50^0c	t/q_t 75^0c	t/q_t 100^0c
10	19.0	18.0	17.4	17.0	0.5263	0.5556	0.5747	0.5882
20	27.0	26.13	25.6	25.2	0.7407	0.7654	0.7813	0.7937
30	38.3	37.27	36.6	36.2	0.7833	0.8049	0.8197	0.8287
40	45.7	44.13	43.2	42.6	0.8753	0.9064	0.9259	0.8287
50	50	79	48.13	47.67	1.0	1.0204	1.0389	1.0489
60	50	49	48.13	47.67	1.20	1.2245	1.2466	1.2587

Intra particles diffusion using activated carbon

Time (min)	q_t(mg/g) 25^0c	q_t(mg/g) 50^0c	q_t(mg/g) 75^0c	q_t(mg/g) 100^0c	$t^1/_2$ 25^0c
10	18.6	17.6	16.8	16.47	3.1623
20	42.0	40.67	39.67	39.0	4.4721
30	34.0	52.8	51.87	51.27	5.4772
40	63.3	60.33	59.53	59.10	6.3246
50	65.0	63.53	62.5	61.87	7.0711
60	65.0	63.53	62.33	61.87	7.7460

Intra particles diffusion using zeolite

Time	q_t(mg/g) 25^0c	q_t(mg/g) 50^0c	q_t(mg/g) 75^0c	q_t(mg/g) 100^0c	$t^1/_2$ 25^0c
10	19.0	18.0	17.4	17.0	3.1623
20	27.0	26.13	25.6	25.2	4.4721
30	38.3	37.27	36.6	36.2	5.4772
40	45.7	44.13	43.2	42.6	6.3246
50	50	49	48.13	47.67	7.0711
60	50	49	48.1	47.67	7.7460

Langmuir isotherm using activated carbon

Time (min)	**q_e (mg/g) 25^{O}C**	**q_e (mg/g) 50^{O}C**	**q_e (mg/g) 75^{O}C**	**q_e (mg/g) 100^{O}C**	**$^{1}/q_e$ 25 ^{O}C**	**$^{1}/q_e$ 50^{O}C**	**$^{1}/q_e$ 75^{O}C**	**$^{1}/q_e$ 100^{O}C**	**$^{1}/_{t}$**
10	18.6	17.6	16.8	16.47	0.0538	0.0568	0.0595	0.0607	0.1
20	42	40.67	39.67	39.0	0.0238	0.0246	0.0252	0.0256	0.05
30	54.0	52.8	51.87	51.27	0.0185	0.0189	0.0193	0.0195	0.033
40	63.3	60.33	59.53	59.10	0.0166	0.0166	0.0166	0.0169	0.025
50	65.0	63.53	62.53	61.87	0.0154	0.0157	0.0160	0.0162	0.02
60	65.0	63.53	62.53	61.87	0.0154	0.0157	0.0160	0.0162	0.0167

Langmuir isotherm using zeolite

Time (min)	**q_e (mg/g) 25^{O}C**	**q_e (mg/g) 50^{O}C**	**q_e (mg/g) 75^{O}C**	**q_e (mg/g) 100^{O}C**	**$^{1}/q_e$ 25 ^{O}C**	**$^{1}/q_e$ 50^{O}C**	**$^{1}/q_e$ 75^{O}C**	**$^{1}/q_e$ 100^{O}C**	**$^{1}/_{t}$**
10	19.0	18.0	17.4	17.0	0.0526	0.0556	0.0575	0.0575	0.100
20	27.0	26.13	25.6	25.2	0.0370	0.0383	0.0391	0.0397	0.050
30	38.3	37.27	36.6	36.2	0.0261	0.0268	0.0273	0.0276	0.033
40	45.7	44.13	43.2	42.6	0.0218	0.0227	0.0231	0.0235	0.025
50	50	49	48.13	47.62	0.020	0.0204	0.0208	0.0210	0.022
60	50	49	48.13	47.67	0.020	0.0204	0.0208	0.0210	0.0167

Frendlich isotherm using activated carbon

Time (min)	Logt	$\log q_t$ 25^{O}C	$\log q_t$ 50^{O}C	$\log q_t$ 75^{O}C	$\log q_t$ 100^{O}C
10	1.000	1.2695	1.2455	1.2253	1.2167
20	1.3010	1.6232	1.6093	1.5985	1.5911
30	1.4771	1.7324	1.7226	1.7149	1.7099
40	1.6021	1.8014	17805	1.7747	1.7716
50	1.6990	1.8129	1.8030	1.7961	1.7915
60	1.7782	1.8129	1.8030	1.7961	1.7915

Frendlich isotherm using zeolite

Time (min)	Logt	$\log q_t$ 25^{O}C	$\log q_t$ 50^{O}C	$\log q_t$ 75^{O}C	$\log q_t$ 100^{O}C
10	1.000	1.2788	1.2553	1.2405	1.2304
20	1.3010	1.4314	1.4171	1.4082	1.4014
30	1.4771	1.5832	1.5714	1.5635	1.5587
40	1.6021	1.6599	1.6447	1.6355	1.6294
50	1.6990	1.6990	1.6902	1.6824	1.6782
60	1.7782	1.6990	1.6902	1.6824	1.6782

Temkin isotherm using activated

Time (min)	q_t(mg/g) 25^{O}C	q_t(mg/g) 50^{O}C	q_t(mg/g) 75^{O}C	q_t(mg/g) 100^{O}C	$t^{1/2}$
10	18.6	17.6	16.8	16.47	2.303
20	42.0	40.67	39.67	39.0	2.996
30	54.0	52.8	51.87	51.27	3.401
40	63.3	60.33	59.53	59.10	3.912
50	65.0	63.5	62.53	61.87	3.912
60	65.0	63.53	62.53	61.87	4.094

Temkin isotherm using zeolite

Time (min)	q_t(mg/g) 25^{O}C	q_t(mg/g) 50^{O}C	q_t(mg/g) 75^{O}C	q_t(mg/g) 100^{O}C	$t^{1/2}$
10	19.0	18.0	17.4	17.0	2.303
20	27.0	26.13	25.6	25.2	2.996
30	38.3	37.27	36.6	36.2	3.401
40	45.7	44.13	43.2	42.6	3.689
50	50	49	48.13	47.67	3.912
60	50	49	48.13	47.67	4.094

APPENDIX B

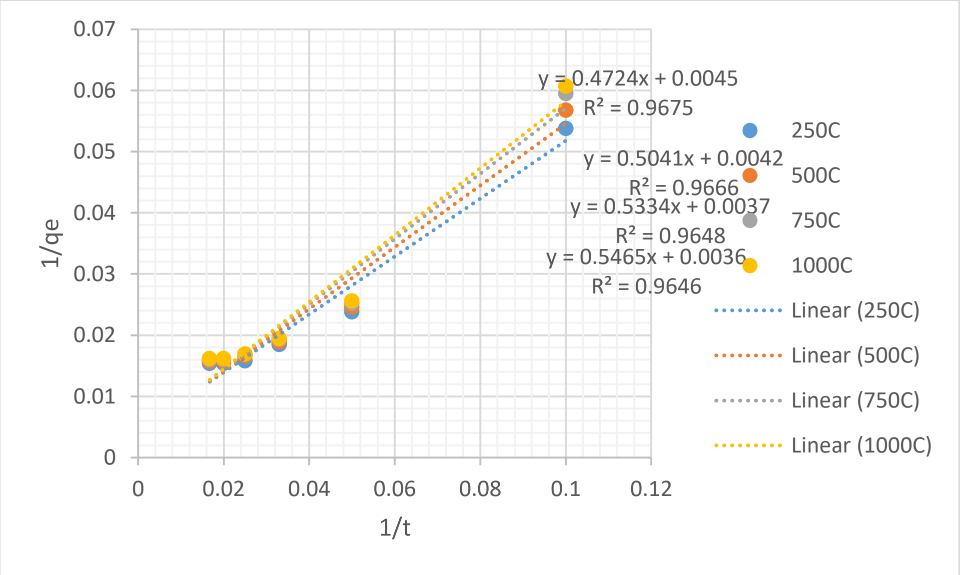

Figure 4.5: Langmuir graph for CO_2 Adsorption using Activated Carbon

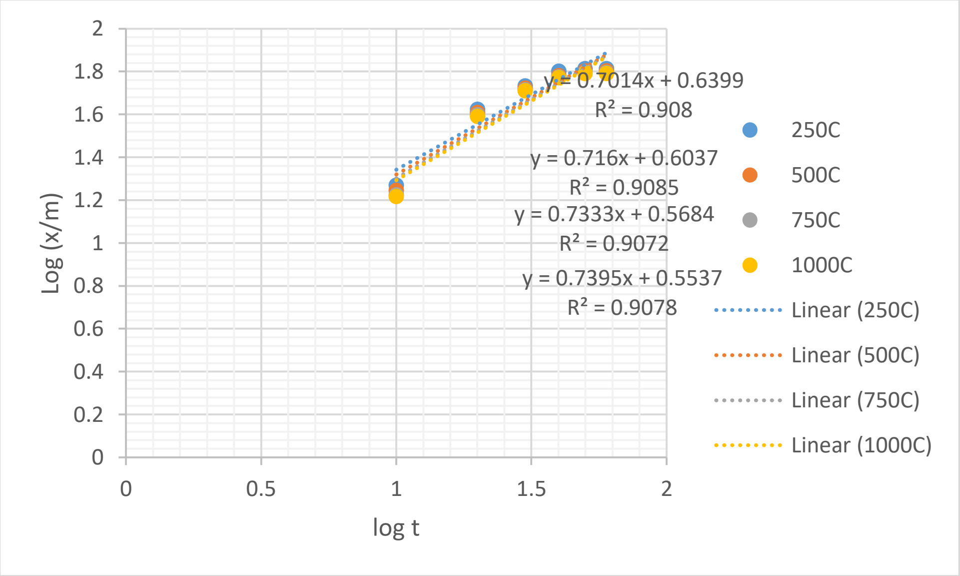

Figure 4.6: Freundlich graph for CO_2 Adsorption using Activated Carbon

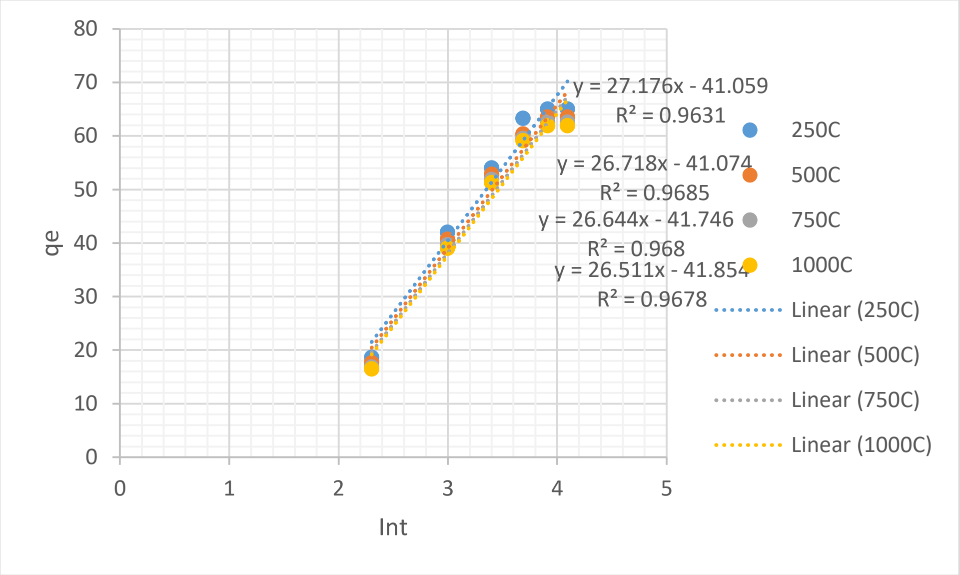

Figure 4.7: Temkin graph for CO_2 Adsorption using Activated Carbon

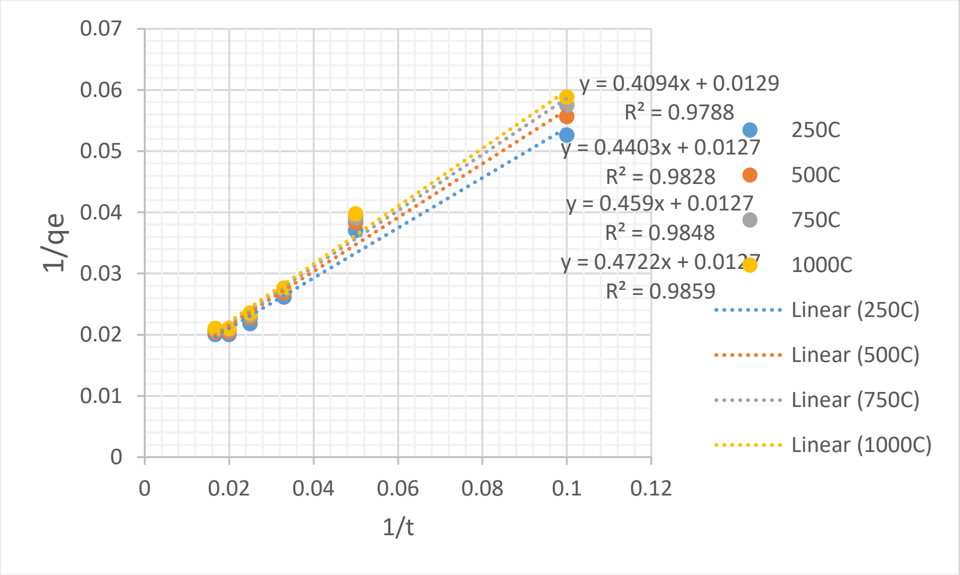

Figure 4.8: Langmuir graph for CO_2 Adsorption using zeolite

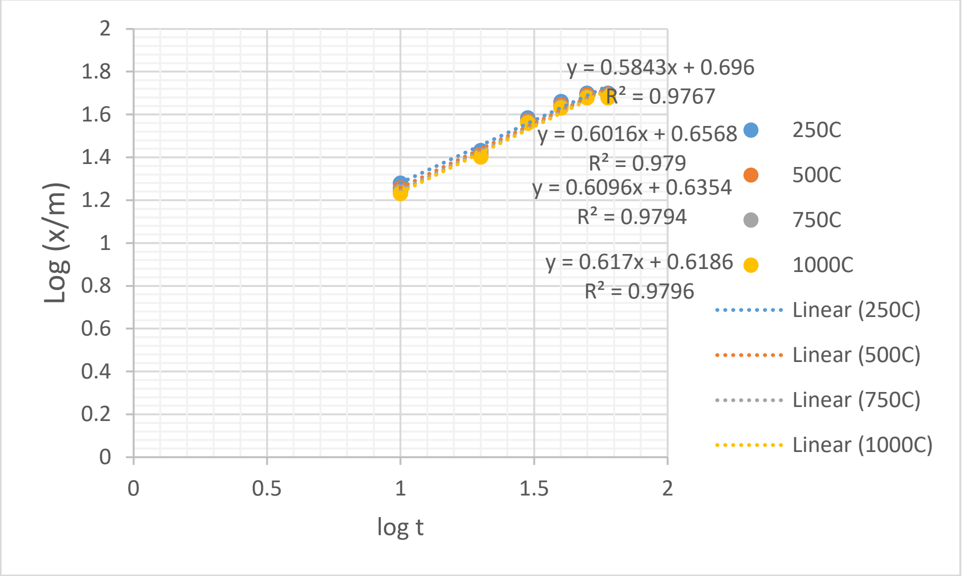

Figure 4.9: Freundlich graph for CO_2 Adsorption using zeolite

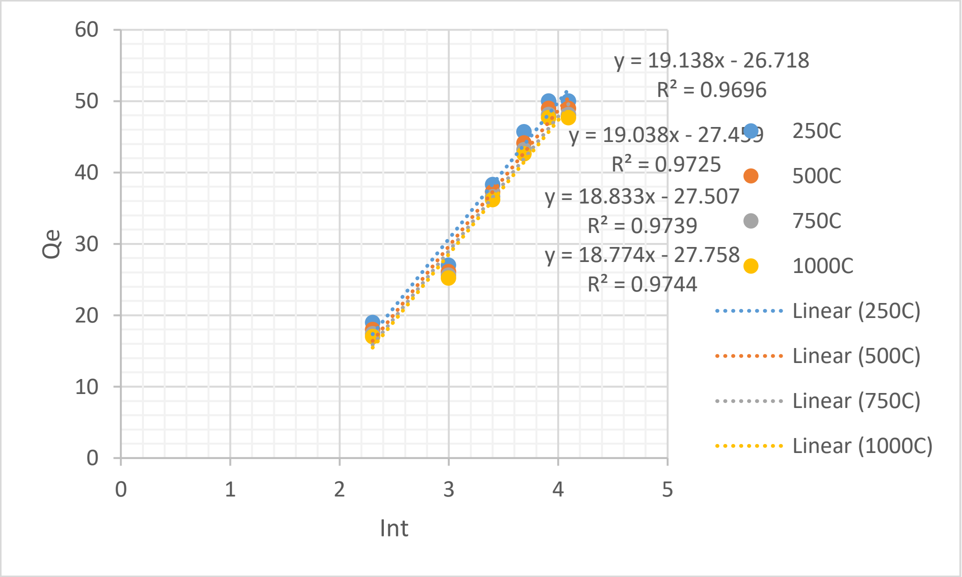

Figure 4.10: Temkin graph for CO_2 Adsorption using zeolite

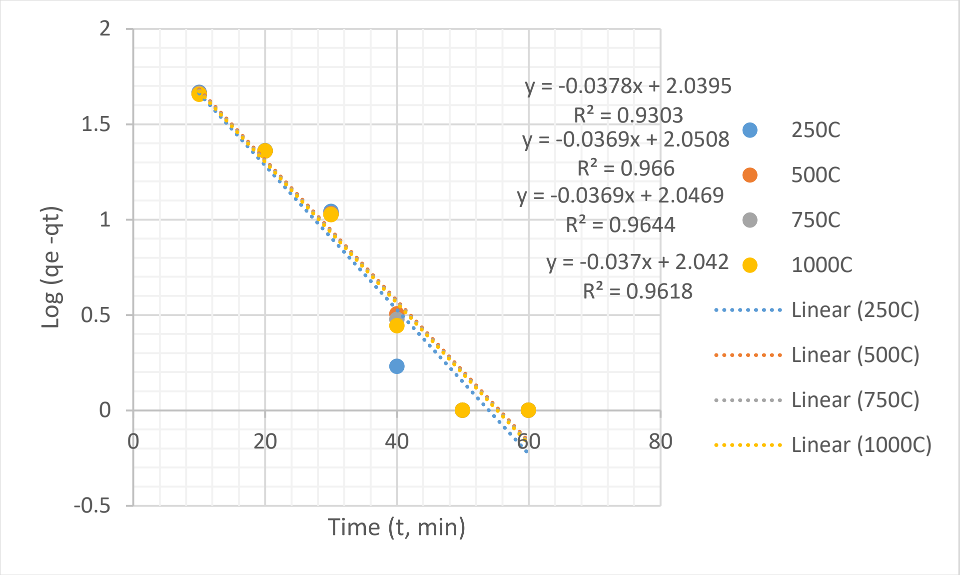

Figure 4.11: Pseudo First Order graph for CO_2 Adsorption using Activated Carbon

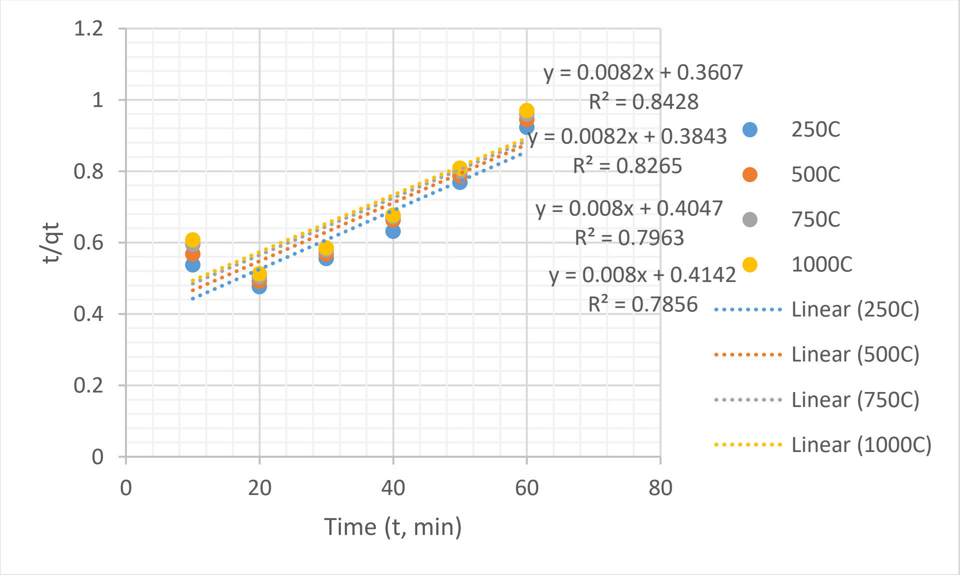

Figure 4.12: Pseudo Second Order graph for CO_2 Adsorption using Activated Carbon

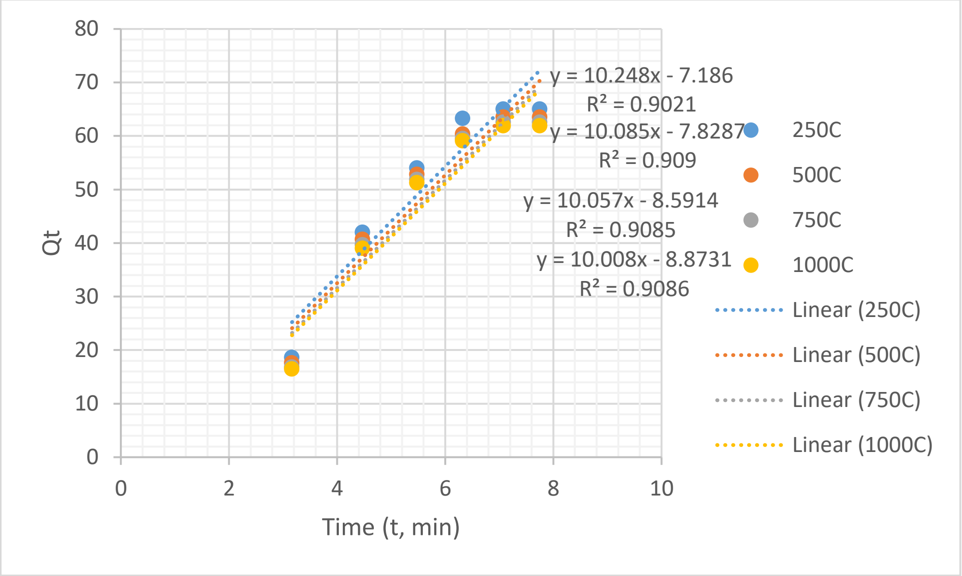

Figure 4.13: Intra particle Diffusion Graph for CO_2 Adsorption using Activated Carbon

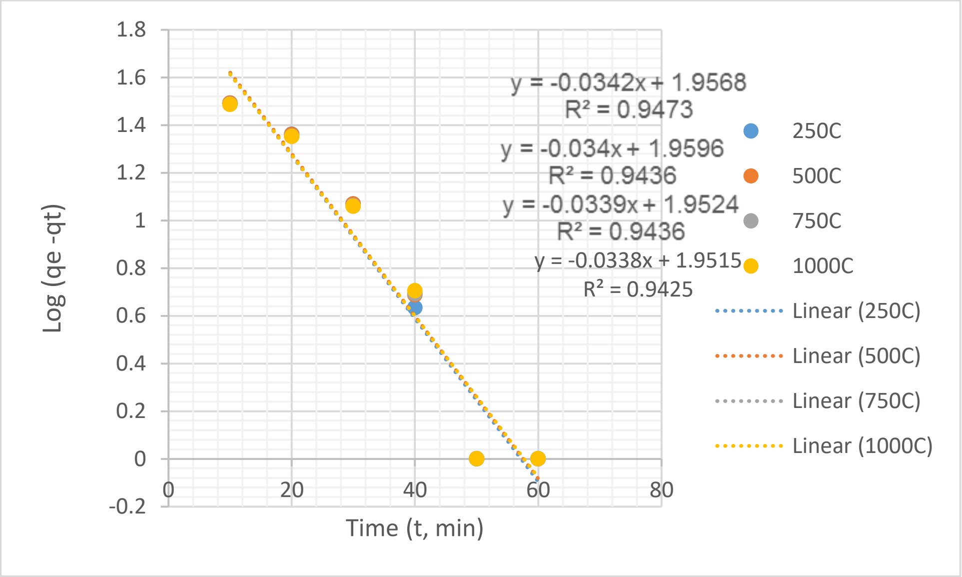

Figure 4.14: Pseudo First Order graph for CO_2 Adsorption using zeolite

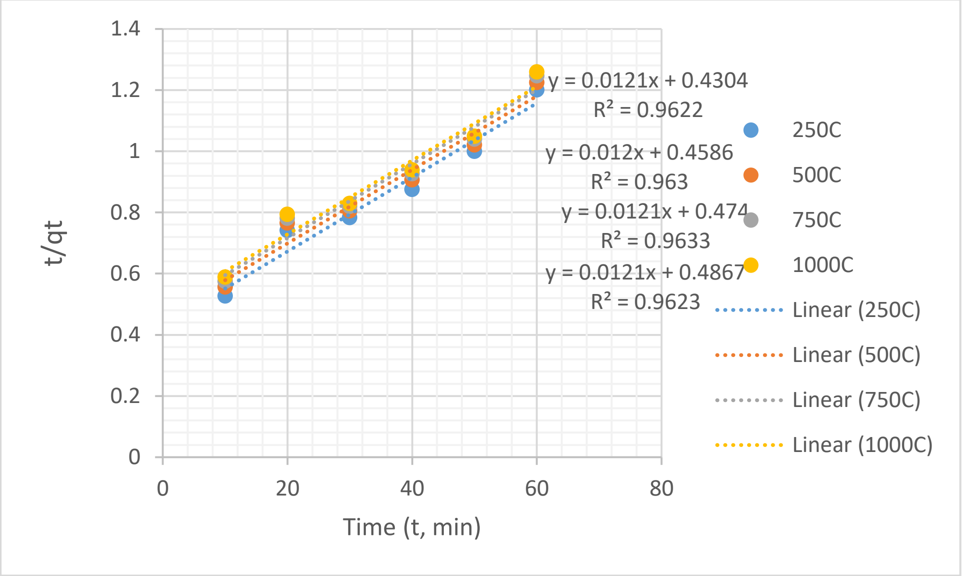

Figure 4.15: Pseudo Second Order graph for CO_2 Adsorption using zeolite

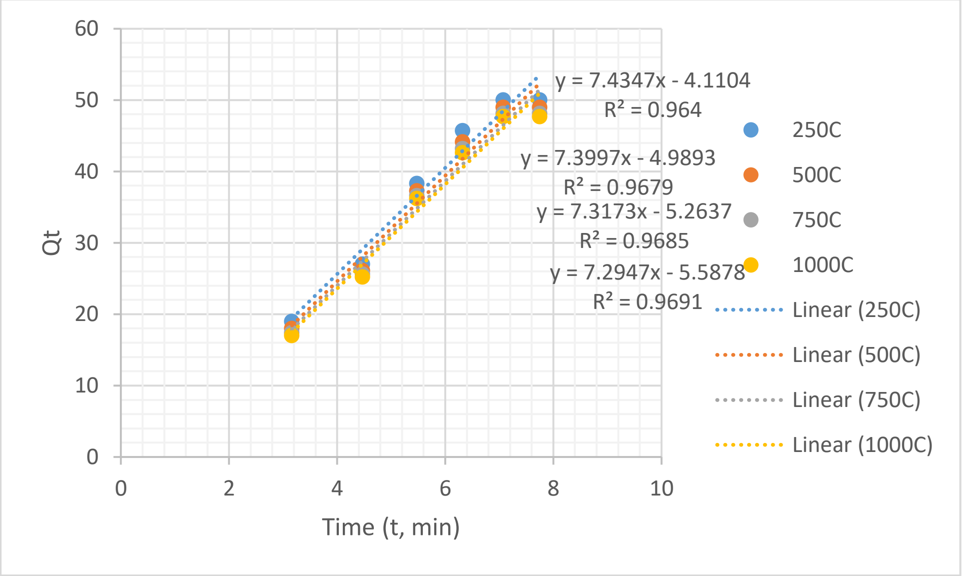

Figure 4.16: Intra particle Diffusion Graph for CO_2 Adsorption using zeolite

APPENDIX C

First order calculation for activate carbon at 25^{O}C

Y = -0.0378$\varkappa$ + 2.0395

Slope = $\frac{K_1}{2.303}$ = -0.0378

K_1 = 0.0871 (min^{-1})

Intercept = log q_e = 2.0395

$Q_e = 10^{2.0395}$

Q_e = 109.5mg/g

At 50^{O}C

y = -0.0369$\varkappa$ + 2.058

slope = $\frac{-K_1}{2.303}$ = -0.0369

K_1 = 0.08498 (min^{-1})

Intercept = log q_e = 2.058

$Q_e = 10^{2.058}$

Q_e = 114.3mg/g

At 75^{O}C

y = -0.0369$\varkappa$ + 2.0469

slope = $\frac{-K_1}{2.303}$ = -0.0369

$K_1 = 0.085\ (\text{min}^{-1})$

Intercept = log q_e = 2.0469

$Q_e = 10^{2.0469}$

Q_e = 111.4mg/g

At 100^{O}C

$y = -0.037\varkappa + 2.042$

slope = $\frac{-K_1}{2.303}$ = -0.037

$K_1 = 0.0852\ (\text{min}^{-1})$

Intercept = log q_e = 2.042

$Q_e = 10^{2.042}$

Q_e = 110.2mg/g

First order calculation for zeolite

At 25^{O}C

$y = -0.0342\varkappa + 1.9568$

slope = $\frac{-K_1}{2.303}$ = -0.0342

$K_1 = 0.07976\ (\text{min}^{-1})$

Intercept = log q_e = 1.9568

$Q_e = 10^{1.9568}$

Q_e = 90.53mg/g

At 50^{O}C

$y = -0.034\varkappa + 1.9596$

slope = $\frac{-K_1}{2.303}$ = -0.034

$K_1 = 0.0783$ (min^{-1})

Intercept = log q_e = 1.9596

$Q_e = 10^{1.9596}$

Q_e = 91.12mg/g

At 75^{O}C

$y = -0.0339\varkappa + 1.9524$

slope = $\frac{-K_1}{2.303}$ = -0.0339

$K_1 = 0.0781$ (min^{-1})

Intercept = log q_e = 1.9524

$Q_e = 10^{1.9524}$

Q_e = 89.62mg/g

At 100^{O}C

$y = -0.0338\varkappa + 1.9515$

slope = $\frac{-K_1}{2.303}$ = -0.0338

$K_1 = 0.0778$ (min^{-1})

Intercept = log q_e = 1.9515

$Q_e = 10^{1.9515}$

Q_e = 89.43mg/g

Second order calculation for activated carbon

At 25^{O}C

y = 0.0082$\varkappa$ + 0.3607

slope = $\frac{-K_1}{q_e}$ = -0.0082

q_e = 121.95mg/g

Intercept = $1/k_2$ l q_e^2 = 0.3607

$\frac{1}{k_2\ (121.95)^2}$ = 0.3607

$k_2 = 1.8644\text{x}10^{-4}$

At 50^{O}C

y = 0.0082$\varkappa$ + 0.3843

slope = $\frac{1}{q_e}$ = 0.0082

q_e = 121mg/g

Intercept = $1/_{k_2}$ q_e^2 = 0.3843

$\frac{1}{k_2\ 122^2}$ = 0.3843

$k_2 = 1.7483\text{x}10^{-4}$

At 75^{O}C

y = 0.008$\varkappa$ + 0.4047

slope = $\frac{1}{q_e}$ = 0.008

q_e = 125mg/g

Intercept = $^1/_{k_2}$ q_e^2 = 0.4047

$\frac{1}{k_2\ (125)^2}$ = 0.4047

k_2 = 1.5814x10^{-4}

At 50^{O}C

y = 0.008$\varkappa$ + 0.4142

slope = $\frac{1}{q_e}$ = 0.008$\varkappa$

q_e = 125mg/g

Intercept = $^1/_{k_2}$ q_e^2 = 0.4142

$\frac{1}{k_2\ 125)^2}$ = 0.4142

k_2 = 1.545x10

Second order calculation for zeolite

At 25^{O}C

$y = 0.0121\varkappa + 0.4304$

slope = $\frac{1}{q_e}$ = 0.0121

q_e = 82.65mg/g

Intercept = $^{1}/_{k_{2\ q_e^2}}$ = 0.4304

$\frac{1}{k_2(82.65)^2}$ = 0.4304

$k_2 = 3.4\text{x}10^{-4}$

At 50^{O}C

$y = 0.0121\varkappa + 0.4586$

slope = $\frac{1}{q_e}$ = 0.012

q_e = 83.33mg/g

Intercept = $\frac{1}{k_2\ q_e^2}$ = 0.4586

$\frac{1}{k_2(83.33)^2}$ = 0.4586

$k_2 = 3.14\text{x}10^{-4}$

At 75^{O}C

y = 0.0121$\varkappa$ + 0.474

slope = $\frac{1}{q_e}$ = 0.0121

q_e = 82.6mg/g

Intercept = $\frac{1}{k_2\ q_e^2}$ = 0.474

$\frac{1}{k_2(82.6)^2}$ = 0.474

$k_2 = 3.092 \times 10^{-4}$

At 100^{O}C

y = 0.0121$\varkappa$ + 0.4867

slope = $\frac{1}{q_e}$ = 0.0121

q_e = 82.6mg/g

Intercept = $\frac{1}{k_2\ q_e^2}$ = 0.4867

$\frac{1}{k_2(82.6)^2}$ = 0.4867

$k_2 = 3.011 \times 10^{-4}$

Intra particle diffusion calculation for activate carbon

At 25^{O}C

$y = 10.248\varkappa – 7.186$

slope = kid = 10.248

c = intercept = 7.186

At 50^{O}C

$y = 10.085\varkappa – 7.8287$

slope = kid = 10.085

c = intercept = 7.8287

At 75^{O}C

$y = 10.057\varkappa – 7.8287$

slope = kid = 10.085

c = intercept = 7.8287

At 100^{O}C

$y = 10.008\varkappa – 8.8731$

slope = 10.008 = kid

c = intercept = 8.8731

Intra particle diffusion calculation for zeolite

At 25^{O}C

$y = 7.4347\varkappa – 4.1104$

slope = kid = 7.4347

c = intercept = 4.1104

At 50^{O}C

$y = 7.3997x - 4.9893$

slope = kid = 7.3997

intercept = c = 4.9893

At 75^{O}C

$y = 7.1173x - 5.2637$

slope = 7.3173 = kid

intercept = c = 5.2637

At 100^{O}C

$y = 7.2947x - 5.5878$

slope = kid = 7.2947

intercept = c = 5.5878

Langmuir isotherm calculation for activated carbon

At 25^{O}C

$y = 0.4724x + 0.0045$

intercept = $\frac{1}{q_e}$ = -0.0045

q_e = 222.2mg/g

slope = $\frac{1}{k_1 q_n}$ = 0.4724

$\frac{1}{k_2\ (222.2)}$ -0.4724

k_1 = 9.53x10^{-3}

At 50^{O}C

y = 0.5041$\varkappa$ + 0.0042

intercept = $\frac{1}{q_e}$ = -0.0042

q_e = 238.1mg/g

slope = $\frac{1}{k_1 q_n}$ = 0.5041

$\frac{1}{k_1\ 2381}$ = 0.5041

k_1 = 8.33x10^{-3}

At 75^{O}C

y = 0.5334$\varkappa$ + 0.0037

intercept = $\frac{1}{q_e}$ = -0.0037

q_e = 270.3mg/g

slope = $\frac{1}{k_1 q_n}$ = 0.5334

$\frac{1}{k_1\ 2703}$ = 0.5334

k_1 = 6.94x10^{-3}

At 100^{O}C

y = 0.5465$\varkappa$ + 0.0036

intercept = $\frac{1}{q_e}$ = -0.0036

q_e = 277.8mg/g

slope = $\frac{1}{k_1 q_n}$ = 0.5465

$\frac{1}{k_1\ 277.8}$ = 0.5465

k_1 = 6.59x10^{-3}

Langmuir Isotherm calculation for zeolite

At 25^{O}C

$y = 0.4094\varkappa + 0.00129$

intercept = $\frac{1}{q_e}$ = -0.0129

q_e = 27.51mg/g

slope = $\frac{1}{k_1 q_n}$ = 0.4094

$\frac{1}{k_1\ 78.74}$ = 0.4094

k_1 = 0.0315(mm^{-1})

At 50^{O}C

$y = 0.4403\varkappa + 0.00127$

intercept = $\frac{1}{q_e}$ = -0.0127

q_e = 78.74mg/g

slope = $\frac{1}{k_1 q_n}$ = 0.4403

$\frac{1}{k_1\ 78.74}$ = 0.4403

k_1 = 0.0288(mm^{-1})

At 75^{O}C

y = 0.459$\varkappa$ + 0.00126

intercept = $\frac{1}{q_e}$ = -0.0126

q_e = 79.365mg/g

slope = $\frac{1}{k_1 q_n}$ = 0.459

$\frac{1}{k_1\ 79.365}$ = 0.459

k_1 = 0.0275(mm^{-1})

At 100^{O}C

y = 0.472$\varkappa$ + 0.00126

intercept = $\frac{1}{q_e}$ = -0.0126

q_e = 79.365mg/g

slope = $\frac{1}{k_1 q_n}$ = 0.472

$\frac{1}{k_1\ 78.365}$ = 0.472

k_1 = 0.0267(mm^{-1})

Frendlich isotherm calculation for activated carbon

At 25^{O}C

$y= 0.7014\varkappa + 0.6399$

slope $=\frac{1}{n} = 0.7014$

n= 1.4257

intercept = $\log k_f = 0.6399$

$k_f =10^{0.6399}$

$= 4.364(\text{min}^{-1})$

At 50^{O}C

$y =0.716 \varkappa + 0.6037$

slope $+ \frac{1}{n} + 0.716$

n= 1.397

intercept = $\log k_f = 0.6037$

$k_f = 10^{0.6037}$

$k_f = 4.015(\text{min}^{-1})$

At 75^{O}C

y =0.7333$\varkappa$ + 0.5684

slope + $\frac{1}{n}$ + 0.7333

n = 1.3637

intercept = logk_f = 0.5684

k_f = $10^{0.5684}$

k_f = 3.7017(min^{-1})

At 100^{O}C

y = 0.7395$\varkappa$ + 0.5537

slope = $\frac{1}{n}$ = 0.7395

n = 1.3523

intercept = logk_f = 0.5537

k_f = $10^{0.5537}$

k_f = 3.5784(min^{-1})

Freundlich isotherm calculation for zeolite

At $25^{O}C$

$y = 0.5843\varkappa + 0.696$

slope = $\frac{1}{n}$ = 0.5843

n = 1.7114

intercept = $\log k_f$ = 0.696

$k_f = 10^{0.696}$

$k_f = 3.966(min^{-1})$

At $50^{O}C$

$y = 0.6016\varkappa + 0.6568$

slope = $\frac{1}{n}$ = 0.6016

n = 1.6222

intercept = $\log k_f$ = 0.6568

$k_f = 10^{0.6568}$

$k_f = 4.5373(min^{-1})$

At 75^{O}C

$y = 0.6096\varkappa + 0.6354$

slope = $\frac{1}{n}$ = 0.6096

n = 1.6404

intercept = $\log k_f$ = 0.6354

$k_f = 10^{0.6354}$

k_f = 4.3192(min^{-1})

At 100^{O}C

$y = 0.617\varkappa + 0.6186$

slope = $\frac{1}{n}$ = 0.617

n = 1.621

intercept = $\log k_f$ = 0.6186

$k_f = 10^{0.6186}$

k_f = 3.1553(min^{-1})

Temkin isotherm calculation for activated carbon

At 25^{O}C

y = 27.176$\varkappa$ - 41.059

intercept = B = 41.059

slope = B in k_t = 27.176

In $k_t = \frac{-27.176}{41.059}$ = -0.6618

$k_1 = \ell^{-0.6618}$

k_t = 0.5159 (min^{-1})

At 50^{O}C

y = 26.718$\varkappa$ - 41.074

intercept = B = 41.074

slope = B in k_t = 26.718

In $k_t = \frac{-27.176}{41.059}$ = -0.65048

$k_1 = \ell^{-0.65048}$

k_t = 0.5218(min^{-1})

At 75^{O}C

$y = 26.644\varkappa - 41.746$

intercept = B = 41.746

slope = B in k_t = 26.644

In $k_t = \frac{-26.644}{41.746} = -0.6382$

$k_1 = \ell^{-0.6382}$

$k_t = 0.5282$

At 100^{O}C

$y = 26.511\varkappa - 41.854$

intercept = B = 41.854

slope = B in k_t = 26.511

In $k_t = \frac{-27.511}{41.854} = -0.6334$

$k_1 = \ell^{-0.6334}$

$k_t = 0.5308(\text{min}^{-1})$

Temkin isotherm calculation for zeolite

At $25^{O}C$

$y = 19.138\varkappa - 26.718$

intercept = B = 26.718

slope = B in k_t = 19.138

In $k_t = \frac{19.138}{26.718} = -0.7163$

$k_1 = \ell^{-0.7163}$

$k_t = 0.4886(min^{-1})$

At $50^{O}C$

$y = 19.038\varkappa - 27.459$

intercept = B = 27.459

slope = B in k_t = 19.038

In $k_t = \frac{19.038}{-27.459} = -0.6933$

$k_1 = \ell^{-0.6933}$

$k_t = 0.4999(min^{-1})$

At 75^{O}C

y = 18.833$\varkappa$ - 27.507

intercept = B = 27.507

slope = B in k_t = 18.833

In $k_t = \frac{18.833}{27.507}$ = -0.68466

$k_1 = \ell^{-0.68466}$

k_t = 0.5043(min^{-1})

Activated energy (E_a) calculation for activated carbon at 298k

$$\text{In } k_2 = \frac{-E_a}{RT} + \text{In } k_1$$

Where:

K_1 is the pseudo first order rate for activated carbon

K_2 is the pseudo second order rate for activated carbon

R is the ideal gas constant

T is temperature at 298k

E_a is the activation energy.

$K_2 = 1.864x10^{-4}min^{-1}$ $k_1 = 0.0871min^{-4}$

$$\text{In } (1.864x10^{-4}) = \frac{-E_a}{8.314x298} + \text{In } (0.0871)$$

$$-8.5975 = \frac{-E_a}{8.314x298} - 2.4407$$

E_a = (8.5973 – 2.4407) 8.314 x 298

E_a = 15.3 KJ/mol.

Activated energy (E_a) calculation for zeolite at 298k

$$\text{In } k_2 = \frac{-E_a}{RT} + \text{In } k_1$$

Where:

K_1 is the pseudo first order rate for zeolite

K_2 is the pseudo second order rate for ZEOLITE

R is the ideal gas constant

T is temperature at 298k

E_a is the activation energy.

$K_2 = 3.4x10^{-4}min^{-1}$, $k_1 = 0.07876min^{-1}$

$$\text{In } (3.4x10^{-1}) = \frac{-E_a}{8.314x298} + \text{In } (0.07876)$$

$$-7.9866 = \frac{-E_a}{8.314x298} - 2.5414$$

E_a = (7.9866 – 2.5414) 8.314 x 298

E_a = 13.5KJ/mol.